Neonatal hyperoxia promotes asthma-like features through IL-33-dependent ILC2 responses

In Su Cheon, PhD[1, 2], Young Min Son, PhD[1, 2], Li Jiang, BS[1, 2], Nicholas P Goplen, PhD[2], Mark H. Kaplan, PhD[1], Andrew H. Limper, MD[2], Hirohito Kita, MD[3], Sophie Paczesny, MD, PhD[1], Y. S. Prakash, MD, PhD [4, 5], Robert Tepper, MD, PhD[1], Shawn K. Ahlfeld, MD[1, 6], and Jie Sun, PhD[1, 2, 3]

1. Department of Pediatrics, Indiana University School of Medicine, Indianapolis, IN 46202
2. Division of Pulmonary and Critical Care Medicine, Department of Medicine, Mayo Clinic College of Medicine and Science, Rochester, MN 55905
3. Department of Immunology, Mayo Clinic College of Medicine and Science, Rochester, MN 55905
4. Department of Anesthesiology, Mayo Clinic College of Medicine and Science, Rochester, MN 55905
5. Department of Physiology and Biomedical Engineering, Mayo Clinic College of Medicine and Science, Rochester, MN 55905
6. Department of Pediatrics, University of Cincinnati, Cincinnati, OH, 45229

Correspondence to Jie Sun. Sun.Jie@mayo.edu

This is the author's manuscript of the article published in final edited form as:

Cheon, I. S., Son, Y. M., Jiang, L., Goplen, N. P., Kaplan, M. H., Limper, A. H., … Sun, J. (2017.). Neonatal hyperoxia promotes asthma-like features through IL-33-dependent ILC2 responses. Journal of Allergy and Clinical Immunology. https://doi.org/10.1016/j.jaci.2017.11.025

ABSTRACT

BACKGROUND:

Premature infants often require oxygen supplementation and, therefore, are exposed to oxidative stress. Following oxygen exposure, preterm infants frequently develop chronic lung disease and have a significantly increased risk of asthma.

OBJECTIVE:

We sought to identify the underlying mechanisms by which neonatal hyperoxia promotes asthma development.

METHODS:

Mice were exposed to neonatal hyperoxia followed by a period room air recovery. A group of mice were also intranasally exposed to house dust mite antigen (HDM). Assessments were performed at various time points for evaluation of airway hyperresponsiveness (AHR), eosinophilia, mucus production, inflammatory gene expression, T helper (Th) and group 2 innate lymphoid cell (ILC2) responses. Sera from term- and preterm-born infants were also collected and the levels of IL-33 and type 2 cytokines were measured.

RESULTS:

Neonatal hyperoxia induced asthma-like features including AHR, mucus hyperplasia, airway eosinophilia, and type 2 pulmonary inflammation. In addition, neonatal hyperoxia promoted allergic Th responses to HDM exposure. Elevated IL-33 levels and ILC2 responses were observed in the lungs most likely due to oxidative stress caused by neonatal hyperoxia. IL-33 receptor signaling and ILC2s were vital for the induction of asthma-like features following neonatal hyperoxia. Serum IL-33 levels correlated significantly with serum levels of IL-5 and IL-13, but not IL-4 in preterm infants.

CONCLUSION:

These data demonstrate that an axis involving IL-33 and ILC2s is important for the development of asthma-like features following neonatal hyperoxia and suggest therapeutic potential for targeting IL-33, ILC2s, and oxidative stress to prevent and/or treat asthma development related to prematurity.

KEY WORDS

Neonatal hyperoxia, Oxidative stress, Asthma, IL-33, ILC2s

CAPSULE SUMMARY

Elevated IL-33 production and enhanced group 2 innate lymphoid cell (ILC2) responses promote the development of asthma-like features related to prematurity and neonatal oxygen exposure

KEY MESSAGES

Neonatal hyperoxia induces the development of asthma-like features in mice

Enhanced IL-33 production and ILC2 responses promote the development of asthma-like features following neonatal hyperoxia

Serum IL-33 levels correlate with IL-5 and IL-13 levels in preterm infants

INTRODUCTION

Preterm birth (born before 37 weeks of gestation) affects about 10% pregnancies [1]. Chronic pulmonary complications of preterm birth are common, and include bronchopulmonary dysplasia (BPD) and asthma [2, 3]. Compared to children born full term, children born significantly preterm had about three times the risk of developing chronic wheezing and asthma disorders later in their lives [4]. The molecular and immunological mechanisms underlying the wheezing and asthma associated with prematurity are currently unclear.

At birth, infants born significantly preterm are likely to require life-supporting respiratory support with positive pressure ventilation and supplemental oxygen. Because the preterm lung is normally developed in a relatively hypoxic intrauterine environment, even exposure to room air (RA, 21% oxygen concentration) is considered hyperoxic and constitutes an oxidative stress [5]. Exposure to higher degrees and durations of hyperoxia results in significant neonatal lung injury, interrupted lung development, and ultimately the development of BPD [6-8]. The lungs of term newborn mice are developmentally and structurally comparable with lungs of human infants born around 26 to 28 weeks' gestation[9]. Therefore hyperoxia exposure of newborn mice offers a useful model for investigating the roles of premature oxygen exposure in regulating lung development and chronic diseases in infants born very prematurely. Using a murine neonatal hyperoxia model, it has been shown that neonatal hyperoxia inhibited the development of alveolar-capillary membrane structure and impaired lung gas-exchange function, similar to findings observed in human BPD [10, 11]. Neonatal hyperoxia also alters lung inflammation status and immune cell compositions [12], which may contribute to the enhanced inflammatory response against influenza virus infection in adult age [13, 14]. In addition, neonatal hyperoxia promotes airway hyperresponsiveness (AHR) to methacholine challenge [15, 16], but the underlying molecular and cellular mechanisms were not investigated.

Innate lymphoid cells (ILCs) have recently been identified as innate counterparts of T helper (Th) cells that are capable of secreting large amounts of cytokines upon stimulation [17]. Based on their cytokine secretion, ILCs can be divided into three groups; group 1 innate lymphoid cells (ILC1s) produce Th1 cytokine IFN-γ, group 2 innate lymphoid cells (ILC2s) produce large amount of IL-5 and IL-13, and group 3 innate lymphoid cells (ILC3s) secret Th17 cytokines IL-17 and IL-22 [17, 18]. In the lungs, ILC2s

appear to be the major ILC subset and respond to epithelial cell-derived cytokines including IL-25, IL-33 and thymic stromal lymphopoietin (TSLP) [19-21]. Enhanced ILC2 activities have been observed in a variety of murine asthma models and human clinical asthma studies [22, 23]. Interestingly, recent evidence shows that ILC2s are accumulated following spontaneous IL-33 release at the alveolar phase of lung development and contribute to the Th2-mediated allergic asthma development later in life [24, 25]. To this end, ILC2s promote antigen uptake and dendritic cell migration to the lung-draining lymph nodes, thereby facilitating the induction of Th2 responses against allergens [24, 26]. Thus ILC2s appear to be one of the key drivers for innate and adaptive immunity in asthma development, particularly at the neonatal stages. However, it remains largely unclear whether neonatal ILC2 development and function are regulated by various external environmental factors (e.g. hyperoxia), thereby influencing the development of pediatric asthma.

We found that neonatal hyperoxia promoted asthma-like immunologic and physiologic features in mice and further enhanced allergic Th2 and Th17 responses in the respiratory tract following allergen exposure. Neonatal hyperoxia promoted IL-33 expression in the developing lungs and enhanced ILC2 expansion was required for the development of asthma-like features. The Nrf2 agonist, sulforaphane (SFN), reduced lung IL-33 levels and ILC2 responses, supporting the role of oxidative stress in the promotion of ILC2s in the lung. Furthermore, genetic ablation of the IL-33 receptor, ST2, decreased asthma-related gene expression, eosinophil recruitment, and ILC2 responses following neonatal hyperoxia. Finally, in preterm infants, we found that serum IL-33 levels positively correlated with serum IL-5 and IL-13, but not IL-4 levels. Our findings suggest that, in infants experiencing oxidative stress as a result of premature birth, IL-33 and ILC2s may play an important role in promoting the development of asthma-related features.

MATERIAL AND METHODS

Ethics statement

All animal experiments were approved by the Institutional Animal Care and U se Committee of Indiana University School of Medicine and the Mayo Clinic.

Blood samples were obtained from infants who were born full term or premature following IRB approval and written parental consent.

Mouse and neonatal hyperoxia model

C57BL/6, *Rag1*$^{-/-}$ and *Rag2/Il2rg*$^{-/-}$ mice were purchased from the Jackson Laboratories (Bar Harbor, ME). *Il1rl1*$^{-/-}$ (ST2-deficient) mice were provided by Dr. McKenzie from MRC Laboratory of Molecular Biology. All mice are in C57BL/6 genetic background. Female mice were primarily used in the study as our own data and previous data have suggested male mice failed to exhibit significantly enhanced AHR following neonatal hyperoxia [15]. The controls of ST2 KO were age-matched C57/BL6 mice. For *Rag2/Il2rg*$^{-/-}$ mice, age-matched C57/BL6 and *Rag1*$^{-/-}$ mice were the controls. For neonatal hyperoxia model, within 24 hours of birth, two or more litters of wild-type C57BL/6 mice were pooled and separated into two equal groups and housed with a single dam in a standard cage. One cage was placed within a 30″ × 20″ × 20″ polypropylene chamber (BioSpherix, Lacona, NY) in which the oxygen concentration was maintained at >80% O_2, and the other was maintained in room air (RA; 21% O_2). Nursing dams were rotated every 24 hours between RA and O_2 groups to avoid oxygen toxicity in dams. Following hyperoxia exposure from postnatal (PN) day PN0-PN7, the mice were returned to room air until sacrifice or HDM challenge. HDM extract (Greer Laboratories, NC) were administrated intranasally (10 μg/20 μl) to mouse 10 times (three times per week) for 4 weeks. After 2 days from the last administration of HDM, mice were sacrificed for cellular analysis. To stimulate Nrf2 activity, mice were intraperitoneal injected with sulforaphane (SFN) at 25 mg/kg daily from PN7 until PN 21.

Measurement of AHR

AHR to methacholine challenged was measured using the FinePoint RC system (Buxco Research Systems, Wilmington, NC) and the airflow was recorded in individual mice according to the manufacturer's guidelines. Briefly, mice were anesthetized and a tracheostomy tube was inserted and connected to a ventilator. After 5 min of stabilization followed by administration of PBS, airway resistance was determined by dose responsiveness to aerosolized methacholine (Sigma-Aldrich, St. Louis, MO) delivered by a nebulizer.

Lung single cell preparation

For airway cells, Broncho-alveolar lavage (BAL) was obtained by flushing the airway multiple times with 400 μl aliquots of sterile PBS, followed by centrifugation to collect airway cells. For lung single cell suspensions, lungs were perfused with PBS, chopped to small pieces using scissors, and digested with 5ml of 183 U/ml collagenase type 2 (Worthington Biochemical Corporation, Lakewood, NJ). After 40 min, lung pieces were dispersed by passage through a 70 μM strainer and RBC lysed with ACK buffer. For cytokine detection in lung, lungs were mechanically separated by passage through a strainer, which was subsequently rinsed with 400 μl of PBS. After centrifugation, supernatants were collected to determine cytokine protein levels by ELISA.

Quantitative RT-PCR

RNA from lung homogenates was isolated using an RNA isolation kit (Sigma-Aldrich) according to the manufacturer's instructions and reverse transcribed into cDNA using random primers (Invitrogen, Grand Island, NY) and MMLV (Invitrogen). cDNAs were amplified using SYBR Green PCR Master Mix (Applied Biosystems, Grand Island, NY) using 7500 Fast-PCR or quantistudio 3 PCR system (Applied Biosystems). Data were generated by the comparative threshold cycle (ΔCT) method by normalizing to hypoxanthine-guanine phosphoribosyltransferase (HPRT).

Epithelial cell culture

Mouse epithelial cells (MLE-12) were and cultured in DMEM/F-12 medium supplemented with 2 % FBS (Hyclone), 1% insulin-Transferrin-Selenium (Gibco), 10 nM hydrocortisone, 10 nM beta-estradiol, L-glutamine 2 mM (Sigma-Aldrich), 10 mM HEPES. To induce oxidative stress, MLE-12 cells were treated with indicated concentrations of H_2O_2 in the presence or absence of 10 μM SFN for 24 hr. Then RNA was extracted for the measurement of *Il33* gene expression. For hyperoxia culture of epithelial cells, MLE-12 cells were cultured in > 70% O_2 concentrations for 24 hours in the presence or absence of SFN (10 μM). Cells were then cultured in normoxia for an additional 24 hours. Il33 gene expression was determined by quantitative RT-PCR.

PCR array

cDNA were obtained from pooled (6-8 lungs) samples per group and mixed with SYBR Green PCR Master Mix. The mixture was used for analysis with mouse asthma and allergy RT^2 PCR array or mouse oxidative stress RT^2 PCR array (Qiagen, Frederick, MD) according to the manufacturer's instructions. Data was analyzed by RT^2 PCR profiler array data analyses software in SABiosciences website.

Determination of ROS levels

To measure intracellular ROS levels in epithelial cells, lung single cell suspensions were surface stained with antibodies conjugated with fluorescence (ant-CD45 and anti-EpCAM) first. Cells were then stained with 10 µM CM-H2DCFDA (Molecular Probes, Carlsbad, CA) at 37°C for 30 min. Cells were washed and analyzed immediately by flow cytometry. Cells that were treated with 50 µM of H_2O_2 served as the positive control.

Flow Cytometry

To quantify ILC2s, lung single cells were stained with fluorescent conjugated lineage markers (Lin: CD11b, CD11c, CD3, B220, Ter-119, Gr-1, NK1.1, TCRβ), anti-Thy1.2, anti-CD25, anti-CD127 and anti-ST2. ILC2s were identified as Lin^- $Th1.2^+$ $CD25^+$ and $CD127^+$. For neutrophil and eosinophil identification, lung or BAL cells were stained with fluorescent conjugated anti-CD45, anti-CD11b, anti-CD11c, anti-Siglec F, anti-Ly6G, and anti-Ly6C. Eosinophils were identified as $CD45^+$ $CD11b^+$ Siglec F^+ and $CD11c^-$, while neutrophils were identified as $CD45^+$ $CD11b^+$ $Ly6G^+$. Total DCs ($CD45^+$, $SiglecF^-$, $Ly6G^-$, $CD11c^{hi}$, MHC II^{hi}), $Fc\varepsilon RI^+$ DCs ($CD45^+$, $SiglecF^-$, $Ly6G^-$, $Fc\varepsilon RI\alpha^+$, $CD11c^{hi}$, HMC II^{hi}), mast cells ($CD45^+$, $SiglecF^-$, $Ly6G^-$, $CD11c^-$, $CD11b^{-/int}$, $Fc\varepsilon RI^+$, c-Kit^+) and basophils ($CD45^+$, $SiglecF^-$, $Ly6G^-$, $CD11c^-$, $CD11b^{-/int}$, $Fc\varepsilon RI^+$, c-Kit^-, $CD49b^+$) were quantified based on the there surface markers indicated above. For intracellular staining, cells were restimulated with 100 ng/ml of PMA (Sigma-Aldrich), 1µg/ml of ionomycin (Sigma-Aldrich) and 40U/ml of hIL-2 in the presence of 1µg/ml of Golgistop (BD Biosciences, San Diego, CA) for 5 hours. Then cells were stained with surface Abs and fixed/permeabilized with BD Cytofix/Cytoperm kit for staining with cytokine Abs. All fluorescent conjugated antibodies were purchased from Biolegend (San Diego, CA), BD Biosciences or eBioscience (San Diego, CA). Samples were acquired through BD LSR II Flow Cytometer (BD Biocience) or Attune NXT flow cytometer (Life technologies). Data were analyzed by using FlowJo software (Treestar, Ashland, OR).

ELISA

Cytokines in the supernatants of lung homogenates were measured with IL-33 ELISA kit (eBioscience) or TSLP ELISA kit (Biolegend) according to the manufacturer's instructions.

Histology

At PN 28, whole lungs were harvested and fixed in 10% formaldehyde (Fisher Scientific, Fair Lawn, NJ) for 48hr and stored in PBS until embedding. Fixed lung tissues were embedded in paraffin, sectioned at 5-μm thickness and stained with hematoxylin and eosin or Periodic Acid Schiff (PAS) by the Indiana University Pathology Laboratory. Histological scores (ranges 1-4) were performed on PAS stained slides blindly by two independent observers. To quantify the percentage of areas stained with PAS within airway epithelium of lung specimens, computer-based image analysis was performed based on a previous report [62]. Briefly, each image was set with scale bar as size per pixel using Image-Pro Premier 3D (Media Cybernetics, Rockville, MD). The areas of airway epithelium and the areas of PAS positive airway epithelium were computer traced based on the differential colored pixels. PAS-positive areas in the epithelium and areas of total airway epithelium were recorded in randomly selected airway sections (~5) per lung tissue section. The percentage of PAS positive area was calculated based on the ratio of PAS positive areas to the total areas of airway epithelium in each lung section.

Clinical samples

Sera were collected from children with at 3 - 30 months of corrected age who were born prematurely (<37 gestation week) or maturely and determined cytokine levels using multiplex (Millipore, Billerica, MA) according to the manufacturer's instructions. All data points are from individual patients.

Statistical Analysis

Data were expressed in mean values ± SEM. One-way ANOVA, two-way ANOVA with subsequent Fisher's LSD test or *t* test were used to determine the significance of differences between groups using GraphPad Prism software. For clinical data, correlations were evaluated by Pearson's test using GraphPad Prism (Graphpad, La Jolla, CA).

RESULTS

Neonatal hyperoxia promotes AHR, mucus production and type 2 airway inflammation

We have utilized a murine neonatal hyperoxia model to replicate the high concentration of oxygen (relative to the hypoxic levels experienced in utero) delivered to lungs of infants born preterm [5, 27]. To mimic the lung injury experienced by preterm infants, for the first 7 postnatal days (PN7) we exposed neonatal mice to either hyperoxia (80% oxygen, O_2) or room air (21% oxygen, RA) (Fig. 1A). To understand the long-term effects of neonatal hyperoxia exposure, all mice were then housed in RA for an additional 21 days and their AHR assessed. Consistent with previous reports [15, 16], we found that

compared to mice raised entirely in RA, mice previously exposed to neonatal hyperoxia showed significantly higher AHR (Fig. 1B). In line with our previous report [28], histological analysis showed that lungs from O_2-exposed mice had simplified alveolar structure (Fig. 1C). Strikingly, neonatal hyperoxia exposure was associated with mucus hyperplasia (Fig. 1C, D, E). In addition, lungs of O_2-exposed mice displayed a significant increase in expression of mucus-associated genes (*Clca1* and *Muc5ac*) (Fig. 1F). The expression of type 2 cytokines IL-5 and IL-13, but not IFN-γ, IL-17 and IL-4, were also significantly increased in the lungs from O_2-exposed mice, suggesting that these mice have enhanced type 2 airway inflammation (Fig. 1G). Further, mice exposed to neonatal hyperoxia also showed airway eosinophilia (Fig. 1H). Interestingly, prior exposure to neonatal hyperoxia was also associated with airway neutrophilia (Fig. 1I). Together, these results demonstrate that neonatal hyperoxia promotes the development of multiple cardinal features of asthma-like symptoms including AHR, mucus production, type 2 inflammation, and recruitment of eosinophils and neutrophils.

Neonatal hyperoxia leads to enhanced lung ILC2 responses at the pediatric stage

We sought to identify the cellular mechanisms underlying the development of AHR and type 2 inflammation associated with prior exposure to neonatal hyperoxia. To quantify IL-13 producing cells, we performed intracellular cytokine staining for single cell suspensions obtained from lungs of RA or O_2-exposed mice. Consistent with our gene expression data (Fig. 1F), compared to those of RA-exposed mice, lungs of O_2 -exposed mice contained a significantly higher proportion of IL-13 producing cells (Fig. 2A, B and C). The majority of the IL-13 producing cells lacked CD4 expression ($CD4^-$) (Fig. 2A, B), indicating they were not Th2 cells. ILC2s are recently-identified, lineage-negative innate immune cells capable of producing large amounts of type 2 cytokines [22]. We found that the majority of lung IL-13 producing cells were lineage-negative (Lin^-) (Fig. 2A, C), suggesting that they are ILC2s. Indeed, these Lin^- IL-13-producing cells also expressed CD25 and CD127 (Fig. S1), further supporting their identity as ILC2s. Extensive surface-marker analysis confirmed the expression of ST2, ICOS, CD90, KLRG1 and low levels of IL-17RB, the typical markers of ILC2s (Fig. 2D). In the lungs from RA or O_2-exposed mice at PN7, the relative frequency and absolute number of ILC2s were not different (Fig. 2E). However, lungs from O_2-exposed mice showed increased ILC2 frequency and/or numbers than those of RA-exposed mice at PN14 and PN28 (Fig. 2E). The levels of lung ILC2 responses were comparable between RA and O_2-exposed mice at PN58 (Fig. 2E). O_2-exposed mice also exhibited enhanced total dendritic cells (DCs), $Fc\varepsilon RI^+$ DCs and basophils in the lungs at PN28 (Fig. S2).

AHR and pulmonary type 2 inflammation are mediated by ILC2s

To determine the roles of ILC2s in the development of AHR and type 2 inflammation, we exposed *Rag1*$^{-/-}$ mice (deficient in T and B cells) and *Rag2*$^{-/-}$/*Il2rg*$^{-/-}$ mice (deficient in T, B and ILCs) to RA or neonatal hyperoxia (as in Fig. 1A) and measured AHR at PN28. Similar to WT mice, O_2-exposed *Rag1*$^{-/-}$ mice showed increased airway responsiveness, suggesting that T and B cells are dispensable for AHR development following neonatal hyperoxia (Fig. 3A). In contrast, O_2-exposed *Rag2*$^{-/-}$ /*Il2rg*$^{-/-}$ mice showed AHR comparable to RA-exposed *Rag1*$^{-/-}$ or *Rag2*$^{-/-}$/*Il2rg*$^{-/-}$ mice, indicating that for AHR development following neonatal hyperoxia ILCs are critical. Compared to those of O_2-exposed *Rag1*$^{-/-}$ mice, histological analysis in the O_2-exposed *Rag2*$^{-/-}$/*Il2rg*$^{-/-}$ mice were comparable to RA-controls and demonstrated diminished airway mucus production (Fig. 3 B, C, D, E). Furthermore, although O_2-exposed *Rag1*$^{-/-}$ mice exhibited increased eosinophilia compared to those of RA-exposed *Rag1*$^{-/-}$ mice, O_2-exposed *Rag2*$^{-/-}$/*Il2rg*$^{-/-}$ mice showed airway eosinophilia similar to those of RA-exposed control mice (*Rag1*$^{-/-}$ or *Rag2*$^{-/-}$/*Il2rg*$^{-/-}$) (Fig. 3F). These data suggest that while Th2 cells are dispensable, ILC2s are essential for the development of neonatal hyperoxia-induced AHR, mucous production, and type 2 inflammation.

Neonatal hyperoxia promotes allergic inflammation

Besides AHR, children and adolescents formerly born preterm exhibit enhanced development of allergic asthma [29]. In addition, pre-clinical murine models have established that ILC2s are capable of enhancing adaptive Th2 responses following intranasal papain challenge [26]. We therefore hypothesized that mice formerly exposed to neonatal hyperoxia would demonstrate elevated allergic responses to subsequent airway allergen exposure. To test this, we administered HDM intranasally (i.n.) to RA- or O_2-exposed WT mice for 4 weeks starting at PN28 and examined Th responses at PN56 (Fig. 4A). We chose PN28 for HDM challenge because maximal differences in ILC2 responses between RA- and O_2-exposed mice were observed at this timepoint (Fig. 2E). As shown previously [30, 31], chronic HDM exposure in both groups increased airway inflammation, eosinophilia and neutrophilia (Fig. 4B). However, HDM-challenged O_2-exposed mice exhibited a significantly exaggerated response as evidenced by higher numbers of airway eosinophils and neutrophils compared to those of HDM-challenged RA-exposed mice. We also observed increased numbers of IL-4, IL-13 and IL-17 producing Lin$^+$ cells present in the airway (Fig. 4C, D) and increased IL-13-producing cells in the lungs (Fig. S3) of HDM-challenged O_2-exposed mice compared to those of HDM-challenged RA-exposed mice. At PN 56, both at baseline (Fig. 2E) and following HDM exposure, the frequencies and absolute numbers of ILC2s between RA- and O_2-exposed groups were not different (Fig. S4). Notably, the majority of the IL-17 producing cells following HDM challenge were Lin$^+$ (Fig. S3), indicating that T cells rather than ILC3s were likely the main IL-17 producing cells

following HDM challenge in both RA and O_2-exposed mice. Together, these data indicate that exposure of neonates to hyperoxia, later exacerbates development of allergic inflammation following respiratory allergen challenge.

Activation of the anti-oxidant pathway attenuates IL-33 and ILC2 responses

To explore the molecular mechanisms that drive enhanced ILC2 responses and type 2 inflammation resulting from neonatal hyperoxia exposure, we examined the expression of epithelial-derived cytokines including IL-25, IL-33 and TSLP, which have been shown to be important for inciting ILC2 responses [20]. In the lungs of O_2-exposed mice at the conclusion of neonatal hyperoxia exposure (PN7) and following 7d of recovery in room air (PN14), mRNA expression of *Tslp* and *Il33* were increased, respectively (Fig. 5A). While TSLP protein levels were undetectable in both RA and O_2-exposed lungs, in the lungs of O_2-exposed mice we verified increased levels of IL-33 protein at PN21 (Fig. 5B). We did not observe measurable IL-33 in bronchoalveolar lavage (BAL) fluid (data not shown), possibly due to the immediate depletion of the low levels of IL-33 produced following O_2-exposure. Hyperoxia can increase oxidative stress via the accumulation of reactive oxygen species (ROS)[32]. We found that oxidative stress genes were upregulated and epithelial cell ROS production was increased in lungs previously exposed to neonatal hyperoxia (Fig. S5 A, B), suggesting that O_2-exposed lungs exhibited increased oxidative stress. To test the hypothesis that oxidative stress facilitates *Il33* expression, we exposed mouse airway epithelial cells to H_2O_2 *in vitro* and then determined *Il33* (Fig. 5C). Treatment with H_2O_2 increased *Il33* expression in epithelial cells (Fig. 5C). Nrf2 is a major transcription factor regulating cellular anti-oxidant responses [33, 34] and its agonist SFN has been used to attenuate oxidative stress and associated inflammation [35, 36]. SFN treatment diminished both basal *Il33* expression and *Il33* upregulation following H_2O_2 exposure, indicating that Nrf2 activation could attenuate *Il33* expression in epithelial cells (Fig. 5D). Consistent with this notion, epithelial cells cultured under hyperoxia conditions exhibited enhanced *Il33* expression *in vitro*, which was dampened by SFN treatment (Fig. 5E). Importantly, treatment of mice with SFN *in vivo* during neonatal hyperoxia attenuated the upregulation of a number of oxidative stress genes (Fig. S5B) and impaired the observed increase in IL-33 protein levels following neonatal hyperoxia (Fig. 5F). IL-33 has been shown to be a major driver of neonatal ILC2 expansion [24]. We therefore examined ILC2 responses following SFN treatment. Although SFN treatment tended to increase baseline ILC2 levels in RA-exposed mice, treatment of SFN in O_2-exposed mice blunted the observed increase in both ILC2s and Lin^-/IL-13 producing cells at PN 28 following hyperoxia (Fig. 5 G, H). Taken together, these data indicated that oxidative stress resulting from neonatal hyperoxia enhances IL-33 expression during recovery, which may contribute to expansion and activation of ILC2s.

ILC2 responses following neonatal hyperoxia are mediated by IL-33 signaling

To determine whether IL-33 signaling is required for type 2 lung inflammation and ILC2 responses following neonatal hyperoxia, we exposed WT and IL-33 receptor-deficient ($ST2^{-/-}$) mice to RA or neonatal hyperoxia (as in Fig. 1A) and assessed lung gene expression and ILC2 responses at PN28 (Fig. 6). Using allergy and asthma PCR-gene array, compared to those of RA-exposed WT mice whole lung RNA from O_2-exposed WT mice showed increased expression of many asthma-related genes. Strikingly, the majority of upregulated genes observed in O_2-exposed WT mice were not upregulated similarly and remained similar to RA-exposed levels in lungs of O_2-exposed *ST2*-deficient mice (Fig. 6A and Fig. S6), suggesting that IL-33 signaling is an important contributor of the altered allergy and asthma gene expression profiles following neonatal hyperoxia. A number of differentially expressed genes including *Arg1, Il21, Il5, Il13, Pmch* and *Rnase2a* were confirmed with RT-PCR (Fig. 6B). Furthermore, compared to those of O_2-exposed WT mice, O_2-exposed ST2-deficient mice showed diminished frequency and numbers of ILC2s in the lungs, suggesting that following neonatal hyperoxia, IL-33 signaling is critical for the expansion of ILC2s (Fig. 6C). Following neonatal hyperoxia, in the absence of IL-33 signaling both IL-13 and IL-5 producing ILC2s were significantly decreased (Fig. 6D). Consistent with diminished ILC2s in the lungs, in response to neonatal hyperoxia ST2-deficient mice failed to develop airway eosinophilia (Fig. 6E). Together, these results suggest that IL-33 signaling via ST2 is critically important for the expression of asthma-related genes, ILC2 responses and airway inflammation following neonatal hyperoxia.

Serum IL-33 levels correlate with IL-5 and IL-13 levels in preterm infants

To determine if the relationship between IL-33 and type 2 cytokines established in the mouse model is conserved in preterm infants, we analyzed the levels of IL-33 and type 2 cytokine concentrations in sera obtained from children (aged 3- 30 months) that had been born either term or preterm (Table S1). Likely due to the limited sample size and varied sample collection timepoint, the levels of IL-33 and type 2 cytokines such as IL-5, IL-13 and IL-4 in the sera of preterm infants were not significantly different with those of term infants (Fig. S7A), although we observed a trend toward increased percentages of individuals having high serum IL-33 levels in preterm infants, particularly in those infants who met criteria for BPD (Fig. S7B). We also observed a trend toward increased percentages of individuals having high serum IL-33 levels in the group of infants born before 30 weeks' gestation (Fig. S7C). Interestingly, there was a significant correlation between serum concentrations of IL-33 and IL-5, and serum concentrations of IL-33 and IL-13 within the preterm group (Fig. 7A, B) but not in term infant group (Fig.

S8). In addition, we found that there were significant correlations between serum IL-33 and IL-13, serum IL-33 and IL-5 levels in sera collected in infants younger than 18 months of age, but not those of sera collected from infants between 18 and 30 months of age (Fig. S9).

Although IL-4 production by ILC2s has been described, unlike IL-13, it is not required for induction of T_H2 responses [26, 37]. We found that serum IL-33 levels did not significantly correlate with serum IL-4 levels in preterm infants (Fig. 7, C). The sum of these clinical data corroborate our findings in the pre-clinical neonatal hyperoxia model: following hyperoxia, we observed increased IL-5 and IL-13 in association with increased IL-33, which is required for ILC2 expansion. Thus, although future studies on respiratory IL-33 and type 2 cytokine levels in preterm infants with larger sample sizes are warranted, these data suggest the proof of principle that an IL-33-ILC2 axis could be a reasonable contributor of asthma-like airway inflammation in preterm infants.

DISCUSSION

Infants born extremely premature often require supplemental oxygen therapy for their survival. However, in preterm infants and in pre-clinical animal models, oxygen supplementation has been associated with interrupted distal lung development, chronic deficits in gas exchange, airway hyper-reactivity, and chronic pulmonary dysfunction [38-40]. Numerous studies have established various detrimental effects of neonatal hyperoxia on lung structural and functional development [27, 41 42]. However, the mechanisms by which neonatal hyperoxia mediates pulmonary inflammation, abnormal lung development, and chronic pulmonary dysfunction are largely unknown. We show here that neonatal hyperoxia enhanced lung IL-33 production and ILC2 responses, thereby resulting in AHR, mucous production and type 2 inflammation. Strikingly, we found that neonatal hyperoxia also exaggerated pulmonary allergic responses to respiratory allergen challenge. Our findings suggest that an axis involving IL-33 and ILC2s is vital for the development of asthma-related pathology following neonatal hyperoxia.

Our observation that young-adult mice previously subjected to neonatal hyperoxia for the first PN7 (the period of saccular and rapid alveolar development) show AHR is in agreement with previous studies of a

similar developmental window [15, 43]. We further demonstrated here that neonatal hyperoxia promoted the development of other asthma-like features including mucus production, airway eosinophilia and neutrophilia and increased expression of type 2 cytokines IL-5 and IL-13. Thus neonatal hyperoxia leads to the development of multiple asthma-like features at the pediatric and young-adult stages. These results are consistent with the data that asthma-like symptoms and AHR are frequently reported in children, adolescents, and young adults that were born very premature and developed BPD [44-46]. Notably, neonatal T cells are prone to developing into Th2-type cells following infection or antigenic challenge via T cell-intrinsic and extrinsic mechanisms[47-49]. It is thus of interest that ILC2s, rather than Th2 cells, are increased in the lungs and required for development of asthma-like symptoms following neonatal hyperoxia. While atopic asthma driven by Th2 cells are responsive to specific antigens or allergens, ILC2s that are driven by hyperoxia are unlikely responsive to specific antigens but driven by cytokines released by reactive epithelial cells. This difference may underlie the fact that some features of asthma and AHR subsequent to extremely premature birth differed from typical allergic childhood asthma [50].

In addition to AHR and type 2 inflammation, we found that neonatal hyperoxia also increased host sensitivity to allergen challenge as reflected by elevated type 2 and type 17 inflammation observed in the lungs following HDM challenge. Notably, previous findings have found that neonatal hyperoxia did not enhance allergic responses to ovalbumin (OVA) challenge [15]. This could be due to the differences in allergens or sensitization routes used as OVA was given through i.p. previously [15], whereas HDM was delivered i.n. in our study. ILC2s have been shown to facilitate sensitization to local, but not systemic, Th2-inducing allergen exposures [51]. Thus, it is possible that enhanced ILC2 responses following neonatal hyperoxia specifically enhance respiratory, but not systemic, allergen sensitization. Consistent with this concept, IL-13-derived from ILC2s was shown to enhance allergic responses through the promotion of dendritic cell migration to lung-draining mediastinal lymph nodes for the priming of naïve CD4 T cells. ILC2s have also been shown to mediate memory Th2 cell activation [52] and can acquire memory-like properties to enhance allergic lung inflammation months after their initial activation [53]. Thus, ILC2s could be a central regulator in the induction of both innate and adaptive immunity during the development of AHR and allergic asthma in response to allergens in infants born prematurely. Future studies are warranted to establish the specific roles and underlying mechanisms by which ILC2s may play to promote Th2 and Th17 responses following neonatal hyperoxia.

Airway epithelial-derived IL-25, TSLP and IL-33 have been shown to enhance ILC2 expansion and/or cytokine production [21, 54-58]. We found that IL-25 expression was comparable between RA and O_2-

exposed mice, suggesting that for the induction of enhanced ILC2 responses following neonatal hyperoxia, IL-25 is unlikely to be vital. Conversely, both TSLP and IL-33 transcription in the lung was enhanced following neonatal hyperoxia. While the effects of TSLP on ILC2 responses are not tested in our study, data observed here have suggested a critical role of IL-33 in promoting ILC2 responses and type 2 inflammation following neonatal hyperoxia, as ST2 deficiency impaired ILC2 expansion and cytokine production. Strikingly, ST2 deficiency diminished the expression of a large numbers of asthma-related genes, indicating that the IL-33-ST2 signaling axis is critical for the development of asthma-like inflammation in the lung following neonatal hyperoxia. Of note, the effects of ST2 signaling in other cell types, including eosinophils, have been documented [59]. Future studies, therefore, are needed to investigate the exact roles of IL-33 signaling in ILC2s in promoting asthma-related gene expression in the lungs. Two recent studies have shown that IL-33 is released spontaneously during lung alveolarization, which drives enhanced ILC2 accumulation and asthma development at the pediatric stage [24, 25]. Our results are consistent with those findings as we also observed that ILC2 percentages in the lungs reached a peak at PN14 in mice housed under room air. However, hyperoxia exposure further enhanced and sustained IL-33 expression, which further promoted and sustained lung ILC2 responses till PN28. Since IL-33 production by epithelial cells is associated with lung remodeling during distal lung development, it is possible that aberrant lung alveolarization and a sustained lung remodeling process may contribute to the prolonged IL-33 expression following neonatal hyperoxia [24].

Our present data lead us to postulate that cellular oxidative stress may be an important factor in the production of IL-33. Increased ROS levels have been shown to contribute significantly to lung injury [60], and Nrf2 agonists given in the course of neonatal hyperoxia have been shown to dampen lung injury and promote normal distal lung development [61]. Consistent with this idea, the Nrf2 agonist, SFN, dampened IL-33 expression *in vitro* and *in vivo* and decreased ILC2s in the lungs of O_2-exposed mice. Interestingly, stimulation of the Nrf2 pathway appeared to elevate ILC2 responses in RA-control mice at baseline. Thus it is plausible that the beneficial effects of SFN on ILC2 responses following neonatal hyperoxia could be partially masked. To this end, a recent paper has suggested that oxidative stress is a key checkpoint for IL-33 release by airway epithelium[62]. Interestingly, due to interruption of placental-fetal transfer and inadequate endogenous production, anti-oxidant responses are compromised in preterm infants [63, 64]. Further, following OVA challenge in the adult age, Nrf2 agonists have been shown to inhibit Th2 responses and asthma development [65]. Thus, targeting oxidative stress with proper anti-oxidants could be a promising method to prevent airflow obstruction and asthma development commonly observed following preterm birth.

As a proof of principle, we measured serum IL-33 and type 2 cytokine levels in older infants formerly born preterm and compared them to age-matched term-born infants. While compared to term infants there is a trend that IL-33 concentrations are elevated in the sera of infants born prematurely, the differences did not reach statistical significance most likely due to the small sample size. However, we observed that there is a significant correlation between serum IL-33 and serum IL-5 and IL-13 levels in preterm infants. Unlike IL-13, ILC2-derived IL-4 is not required to induce T_H2 responses [26]. Thus, these data provide a proof of principle that IL-33-driven ILC2s responses may be relevant in the development of asthma-like symptoms observed in those of preterm infants. Indeed, IL-33 has been increasingly appreciated as a major driver of human asthma [66, 67]. Notably, IL-33 activity is regulated by multiple posttranslational events including protease cleavage and oxidization [68]. The IL-33 levels measured here did not differentiate the active versus non-active forms. Furthermore, we measured circulating rather than respiratory IL-33 due to the lack of accessibility to respiratory samples. In order to firmly establish the roles of IL-33 in asthma development in preterm infants, active forms of respiratory IL-33 levels should be analyzed in the future.

Extremely preterm infants in the post-surfactant era are exposed to lower degrees of hyperoxia than previously. Therefore, given the significant change in clinical practice and disease phenotype, animal models utilizing excessive hyperoxia should be assessed for their clinical-relevance. We chose to use 80% oxygen because, as we have previously published, similar levels of hyperoxia produce a durable phenotype that structurally and functionally mimics many of the aspects of post-surfactant BPD [11, 28]. Recent clinical reports of extremely premature infants have consistently suggested a dose-response effect with oxygen support and lung function. For example, in infants and children previously diagnosed with BPD, the duration of oxygen supplementation and deficits in FEV1 and DLco were positively correlated [6, 69, 70]. Likewise, the severity of BPD and the degree of persistent lung dysfunction are also positively correlated [71-73]. Indeed, even in premature infants that did not develop BPD, early, cumulative oxygen exposure is predictive of persistent pulmonary dysfunction [7]. Although present-day neonatal care strives to reduce oxygen exposure to the lowest effective dose, many infants with significant early and persistent lung disease are routinely exposed to 40-50% oxygen on average, and many are exposed to 60-70% or higher [74-77]. Thus, while careful oxygen titration has emerged as a centerpiece of neonatal care, many infants continue to require excessive oxygen supplementation, the degree of which generally correlates with persistent lung dysfunction. As with any animal model, direct comparison to the human condition is often complex. Given that the murine lung is designed to develop in an environment that is relatively hyperoxic compared to the human lung at the same stage, it is likely that higher levels of hyperoxia are

required to injure the murine lung to a similar degree. While we have not systematically investigated the above-mentioned possibilities, we justify our use of the current model based on its ability to phenocopy some of the hallmark structural and functional characteristics of present-day BPD [11, 28].

In conclusion, our studies have revealed that neonatal hyperoxia promotes the development of asthma-like features and enhances host reactivity to respiratory allergen. We thus have provided viable cellular and molecular mechanisms explaining enhanced asthma development in children born prematurely. Our results suggest targeting the IL-33 and ILC2 axis may be a reasonable future approach to prevent asthma development and/or treat asthma-like symptoms in children born prematurely.

ACKNOWLEDGMENTS

This study was supported by RO1 AI112844, AG047156 and HL126647 to J.S.; R01 AI095282, AI129241 and HL62150 to M.H.K.; RO1 HL62150 and Huvis Foundation grant to A. H. L; RO1 HL117823 and RO1 AI128729 to H. K.; R01 CA168814 to S. P.; Indiana Pediatric Scientist Award and K12 HD068371 to S. K.A; RO1 HL056470 to Y.S.P. We thank Dr. Andrew McKenzie for ST2-deficient mice. We thank nurses and physicians at IU Riley Hospital for collecting infant sera.

REFERENCES:

1. Rubens CE, Sadovsky Y, Muglia L, Gravett MG, Lackritz E, Gravett C. Prevention of preterm birth: harnessing science to address the global epidemic. Science translational medicine 2014; 6:262sr5.
2. Jensen EA, Schmidt B. Epidemiology of bronchopulmonary dysplasia. Birth defects research. Part A, Clinical and molecular teratology 2014; 100:145-57.
3. Halterman JS, Lynch KA, Conn KM, Hernandez TE, Perry TT, Stevens TP. Environmental exposures and respiratory morbidity among very low birth weight infants at 1 year of life. Archives of disease in childhood 2009; 94:28-32.
4. Been JV, Lugtenberg MJ, Smets E, van Schayck CP, Kramer BW, Mommers M, et al. Preterm birth and childhood wheezing disorders: a systematic review and meta-analysis. PLoS medicine 2014; 11:e1001596.
5. Vogel ER, Britt RD, Jr., Trinidad MC, Faksh A, Martin RJ, MacFarlane PM, et al. Perinatal oxygen in the developing lung. Canadian journal of physiology and pharmacology 2015; 93:119-27.
6. Cazzato S, Ridolfi L, Bernardi F, Faldella G, Bertelli L. Lung function outcome at school age in very low birth weight children. Pediatric pulmonology 2013; 48:830-7.
7. Stevens TP, Dylag A, Panthagani I, Pryhuber G, Halterman J. Effect of cumulative oxygen exposure on respiratory symptoms during infancy among VLBW infants without bronchopulmonary dysplasia. Pediatric pulmonology 2010; 45:371-9.

8. Laughon MM, Langer JC, Bose CL, Smith PB, Ambalavanan N, Kennedy KA, et al. Prediction of bronchopulmonary dysplasia by postnatal age in extremely premature infants. American journal of respiratory and critical care medicine 2011; 183:1715-22.
9. Rieger-Fackeldey E, Park MS, Schanbacher BL, Joshi MS, Chicoine LG, Nelin LD, et al. Lung development alterations in newborn mice after recovery from exposure to sublethal hyperoxia. The American journal of pathology 2014; 184:1010-6.
10. Dauger S, Ferkdadji L, Saumon G, Vardon G, Peuchmaur M, Gaultier C, et al. Neonatal exposure to 65% oxygen durably impairs lung architecture and breathing pattern in adult mice. Chest 2003; 123:530-8.
11. Ahlfeld SK, Gao Y, Conway SJ, Tepper RS. Relationship of structural to functional impairment during alveolar-capillary membrane development. The American journal of pathology 2015; 185:913-9.
12. Liao J, Kapadia VS, Brown LS, Cheong N, Longoria C, Mija D, et al. The NLRP3 inflammasome is critically involved in the development of bronchopulmonary dysplasia. Nature communications 2015; 6:8977.
13. O'Reilly MA, Marr SH, Yee M, McGrath-Morrow SA, Lawrence BP. Neonatal hyperoxia enhances the inflammatory response in adult mice infected with influenza A virus. American journal of respiratory and critical care medicine 2008; 177:1103-10.
14. Yee M, Chess PR, McGrath-Morrow SA, Wang Z, Gelein R, Zhou R, et al. Neonatal oxygen adversely affects lung function in adult mice without altering surfactant composition or activity. American journal of physiology. Lung cellular and molecular physiology 2009; 297:L641-9.
15. Regal JF, Lawrence BP, Johnson AC, Lojovich SJ, O'Reilly MA. Neonatal oxygen exposure alters airway hyper-responsiveness but not the response to allergen challenge in adult mice. Pediatric allergy and immunology : official publication of the European Society of Pediatric Allergy and Immunology 2014; 25:180-6.
16. Kumar VH, Lakshminrusimha S, Kishkurno S, Paturi BS, Gugino SF, Nielsen L, et al. Neonatal hyperoxia increases airway reactivity and inflammation in adult mice. Pediatric pulmonology 2016; 51:1131-41.
17. Gasteiger G, Rudensky AY. Interactions between innate and adaptive lymphocytes. Nature reviews. Immunology 2014; 14:631-9.
18. Artis D, Spits H. The biology of innate lymphoid cells. Nature 2015; 517:293-301.
19. Neill DR, Wong SH, Bellosi A, Flynn RJ, Daly M, Langford TK, et al. Nuocytes represent a new innate effector leukocyte that mediates type-2 immunity. Nature 2010; 464:1367-70.
20. Martinez-Gonzalez I, Steer CA, Takei F. Lung ILC2s link innate and adaptive responses in allergic inflammation. Trends in immunology 2015; 36:189-95.
21. Stier MT, Bloodworth MH, Toki S, Newcomb DC, Goleniewska K, Boyd KL, et al. Respiratory syncytial virus infection activates IL-13-producing group 2 innate lymphoid cells through thymic stromal lymphopoietin. The Journal of allergy and clinical immunology 2016; 138:814-24 e11.
22. Klein Wolterink RG, Kleinjan A, van Nimwegen M, Bergen I, de Bruijn M, Levani Y, et al. Pulmonary innate lymphoid cells are major producers of IL-5 and IL-13 in murine models of allergic asthma. European journal of immunology 2012; 42:1106-16.
23. Smith SG, Chen R, Kjarsgaard M, Huang C, Oliveria JP, O'Byrne PM, et al. Increased numbers of activated group 2 innate lymphoid cells in the airways of patients with severe asthma and persistent airway eosinophilia. The Journal of allergy and clinical immunology 2016; 137:75-86 e8.
24. de Kleer IM, Kool M, de Bruijn MJ, Willart M, van Moorleghem J, Schuijs MJ, et al. Perinatal Activation of the Interleukin-33 Pathway Promotes Type 2 Immunity in the Developing Lung. Immunity 2016; 45:1285-98.

25. Steer CA, Martinez-Gonzalez I, Ghaedi M, Allinger P, Matha L, Takei F. Group 2 innate lymphoid cell activation in the neonatal lung drives type 2 immunity and allergen sensitization. The Journal of allergy and clinical immunology 2017.
26. Halim TY, Steer CA, Matha L, Gold MJ, Martinez-Gonzalez I, McNagny KM, et al. Group 2 innate lymphoid cells are critical for the initiation of adaptive T helper 2 cell-mediated allergic lung inflammation. Immunity 2014; 40:425-35.
27. Domm W, Misra RS, O'Reilly MA. Affect of Early Life Oxygen Exposure on Proper Lung Development and Response to Respiratory Viral Infections. Frontiers in medicine 2015; 2:55.
28. Cox AM, Gao Y, Perl AT, Tepper RS, Ahlfeld SK. Cumulative effects of neonatal hyperoxia on murine alveolar structure and function. Pediatric pulmonology 2017; 52:616-24.
29. Goncalves C, Wandalsen G, Lanza F, Goulart AL, Sole D, Dos Santos A. Repercussions of preterm birth on symptoms of asthma, allergic diseases and pulmonary function, 6-14 years later. Allergologia et immunopathologia 2016; 44:489-96.
30. Tashiro H, Takahashi K, Hayashi S, Kato G, Kurata K, Kimura S, et al. Interleukin-33 from Monocytes Recruited to the Lung Contributes to House Dust Mite-Induced Airway Inflammation in a Mouse Model. PloS one 2016; 11:e0157571.
31. Lei Y, Boinapally V, Zoltowska A, Adner M, Hellman L, Nilsson G. Vaccination against IL-33 Inhibits Airway Hyperresponsiveness and Inflammation in a House Dust Mite Model of Asthma. PloS one 2015; 10:e0133774.
32. Bouch S, O'Reilly M, Harding R, Sozo F. Neonatal exposure to mild hyperoxia causes persistent increases in oxidative stress and immune cells in the lungs of mice without altering lung structure. American journal of physiology. Lung cellular and molecular physiology 2015; 309:L488-96.
33. Nguyen T, Nioi P, Pickett CB. The Nrf2-antioxidant response element signaling pathway and its activation by oxidative stress. The Journal of biological chemistry 2009; 284:13291-5.
34. Espinosa-Diez C, Miguel V, Mennerich D, Kietzmann T, Sanchez-Perez P, Cadenas S, et al. Antioxidant responses and cellular adjustments to oxidative stress. Redox biology 2015; 6:183-97.
35. Tanito M, Masutani H, Kim YC, Nishikawa M, Ohira A, Yodoi J. Sulforaphane induces thioredoxin through the antioxidant-responsive element and attenuates retinal light damage in mice. Investigative ophthalmology & visual science 2005; 46:979-87.
36. McGrath-Morrow SA, Lauer T, Collaco JM, Lopez A, Malhotra D, Alekseyev YO, et al. Transcriptional responses of neonatal mouse lung to hyperoxia by Nrf2 status. Cytokine 2014; 65:4-9.
37. Noval Rivas M, Burton OT, Oettgen HC, Chatila T. IL-4 production by group 2 innate lymphoid cells promotes food allergy by blocking regulatory T-cell function. The Journal of allergy and clinical immunology 2016; 138:801-11 e9.
38. Giannandrea M, Yee M, O'Reilly MA, Lawrence BP. Memory CD8+ T cells are sufficient to alleviate impaired host resistance to influenza A virus infection caused by neonatal oxygen supplementation. Clinical and vaccine immunology : CVI 2012; 19:1432-41.
39. Fawke J, Lum S, Kirkby J, Hennessy E, Marlow N, Rowell V, et al. Lung function and respiratory symptoms at 11 years in children born extremely preterm: the EPICure study. American journal of respiratory and critical care medicine 2010; 182:237-45.
40. Jaakkola JJ, Ahmed P, Ieromnimon A, Goepfert P, Laiou E, Quansah R, et al. Preterm delivery and asthma: a systematic review and meta-analysis. The Journal of allergy and clinical immunology 2006; 118:823-30.
41. O'Reilly M, Sozo F, Harding R. Impact of preterm birth and bronchopulmonary dysplasia on the developing lung: long-term consequences for respiratory health. Clinical and experimental pharmacology & physiology 2013; 40:765-73.
42. Ahlfeld SK, Conway SJ. Assessment of inhibited alveolar-capillary membrane structural development and function in bronchopulmonary dysplasia. Birth defects research. Part A, Clinical and molecular teratology 2014; 100:168-79.

43. Wang H, Jafri A, Martin RJ, Nnanabu J, Farver C, Prakash YS, et al. Severity of neonatal hyperoxia determines structural and functional changes in developing mouse airway. American journal of physiology. Lung cellular and molecular physiology 2014; 307:L295-301.
44. Vollsaeter M, Roksund OD, Eide GE, Markestad T, Halvorsen T. Lung function after preterm birth: development from mid-childhood to adulthood. Thorax 2013; 68:767-76.
45. Gibson AM, Doyle LW. Respiratory outcomes for the tiniest or most immature infants. Seminars in fetal & neonatal medicine 2014; 19:105-11.
46. Islam JY, Keller RL, Aschner JL, Hartert TV, Moore PE. Understanding the Short- and Long-Term Respiratory Outcomes of Prematurity and Bronchopulmonary Dysplasia. American journal of respiratory and critical care medicine 2015; 192:134-56.
47. Lewis DB, Gern JE, Hill HR, Friedlander SL, La Pine TR, Lemanske RF, Jr., et al. Newborn immunology: relevance to the clinician. Current problems in pediatric and adolescent health care 2006; 36:189-204.
48. Hong JY, Bentley JK, Chung Y, Lei J, Steenrod JM, Chen Q, et al. Neonatal rhinovirus induces mucous metaplasia and airways hyperresponsiveness through IL-25 and type 2 innate lymphoid cells. The Journal of allergy and clinical immunology 2014; 134:429-39.
49. Saravia J, You D, Shrestha B, Jaligama S, Siefker D, Lee GI, et al. Respiratory Syncytial Virus Disease Is Mediated by Age-Variable IL-33. PLoS pathogens 2015; 11:e1005217.
50. Halvorsen T, Skadberg BT, Eide GE, Roksund O, Aksnes L, Oymar K. Characteristics of asthma and airway hyper-responsiveness after premature birth. Pediatric allergy and immunology : official publication of the European Society of Pediatric Allergy and Immunology 2005; 16:487-94.
51. Gold MJ, Antignano F, Halim TY, Hirota JA, Blanchet MR, Zaph C, et al. Group 2 innate lymphoid cells facilitate sensitization to local, but not systemic, TH2-inducing allergen exposures. The Journal of allergy and clinical immunology 2014; 133:1142-8.
52. Halim TY, Hwang YY, Scanlon ST, Zaghouani H, Garbi N, Fallon PG, et al. Group 2 innate lymphoid cells license dendritic cells to potentiate memory TH2 cell responses. Nature immunology 2016; 17:57-64.
53. Martinez-Gonzalez I, Matha L, Steer CA, Ghaedi M, Poon GF, Takei F. Allergen-Experienced Group 2 Innate Lymphoid Cells Acquire Memory-like Properties and Enhance Allergic Lung Inflammation. Immunity 2016; 45:198-208.
54. Divekar R, Kita H. Recent advances in epithelium-derived cytokines (IL-33, IL-25, and thymic stromal lymphopoietin) and allergic inflammation. Current opinion in allergy and clinical immunology 2015; 15:98-103.
55. Kumar RK, Foster PS, Rosenberg HF. Respiratory viral infection, epithelial cytokines, and innate lymphoid cells in asthma exacerbations. Journal of leukocyte biology 2014; 96:391-6.
56. Barlow JL, Peel S, Fox J, Panova V, Hardman CS, Camelo A, et al. IL-33 is more potent than IL-25 in provoking IL-13-producing nuocytes (type 2 innate lymphoid cells) and airway contraction. The Journal of allergy and clinical immunology 2013; 132:933-41.
57. Monticelli LA, Buck MD, Flamar AL, Saenz SA, Tait Wojno ED, Yudanin NA, et al. Arginase 1 is an innate lymphoid-cell-intrinsic metabolic checkpoint controlling type 2 inflammation. Nature immunology 2016; 17:656-65.
58. Moro K, Yamada T, Tanabe M, Takeuchi T, Ikawa T, Kawamoto H, et al. Innate production of T(H)2 cytokines by adipose tissue-associated c-Kit(+)Sca-1(+) lymphoid cells. Nature 2010; 463:540-4.
59. Johnston LK, Hsu CL, Krier-Burris RA, Chhiba KD, Chien KB, McKenzie A, et al. IL-33 Precedes IL-5 in Regulating Eosinophil Commitment and Is Required for Eosinophil Homeostasis. Journal of immunology 2016; 197:3445-53.
60. Datta A, Kim GA, Taylor JM, Gugino SF, Farrow KN, Schumacker PT, et al. Mouse lung development and NOX1 induction during hyperoxia are developmentally regulated and

mitochondrial ROS dependent. American journal of physiology. Lung cellular and molecular physiology 2015; 309:L369-77.

61. Ni J, Lin YG, Wu L, Huang W, Wei JF, Jiang XQ. [Protective Effect of Activated Nrf2 against Hyperoxia-induced Lung Injury in Neonatal Rats]. Sichuan da xue xue bao. Yi xue ban = Journal of Sichuan University. Medical science edition 2015; 46:399-402.
62. Uchida M, Anderson EL, Squillace DL, Patil N, Maniak PJ, Iijima K, et al. Oxidative stress serves as a key checkpoint for IL-33 release by airway epithelium. Allergy 2017.
63. Poggi C, Dani C. Antioxidant strategies and respiratory disease of the preterm newborn: an update. Oxidative medicine and cellular longevity 2014; 2014:721043.
64. Asikainen TM, White CW. Antioxidant defenses in the preterm lung: role for hypoxia-inducible factors in BPD? Toxicology and applied pharmacology 2005; 203:177-88.
65. Rangasamy T, Guo J, Mitzner WA, Roman J, Singh A, Fryer AD, et al. Disruption of Nrf2 enhances susceptibility to severe airway inflammation and asthma in mice. The Journal of experimental medicine 2005; 202:47-59.
66. Gluck J, Rymarczyk B, Kasprzak M, Rogala B. Increased Levels of Interleukin-33 and Thymic Stromal Lymphopoietin in Exhaled Breath Condensate in Chronic Bronchial Asthma. International archives of allergy and immunology 2016; 169:51-6.
67. Guo Z, Wu J, Zhao J, Liu F, Chen Y, Bi L, et al. IL-33 promotes airway remodeling and is a marker of asthma disease severity. The Journal of asthma : official journal of the Association for the Care of Asthma 2014; 51:863-9.
68. Cohen ES, Scott IC, Majithiya JB, Rapley L, Kemp BP, England E, et al. Oxidation of the alarmin IL-33 regulates ST2-dependent inflammation. Nature communications 2015; 6:8327.
69. Jacob SV, Coates AL, Lands LC, MacNeish CF, Riley SP, Hornby L, et al. Long-term pulmonary sequelae of severe bronchopulmonary dysplasia. J Pediatr 1998; 133:193-200.
70. Doyle LW, Carse E, Adams AM, Ranganathan S, Opie G, Cheong JLY, et al. Ventilation in Extremely Preterm Infants and Respiratory Function at 8 Years. N Engl J Med 2017; 377:329-37.
71. Keller RL, Feng R, DeMauro SB, Ferkol T, Hardie W, Rogers EE, et al. Bronchopulmonary Dysplasia and Perinatal Characteristics Predict 1-Year Respiratory Outcomes in Newborns Born at Extremely Low Gestational Age: A Prospective Cohort Study. J Pediatr 2017; 187:89-97 e3.
72. Ronkainen E, Dunder T, Peltoniemi O, Kaukola T, Marttila R, Hallman M. New BPD predicts lung function at school age: Follow-up study and meta-analysis. Pediatr Pulmonol 2015; 50:1090-8.
73. Mourani PM, Sontag MK, Younoszai A, Miller JI, Kinsella JP, Baker CD, et al. Early pulmonary vascular disease in preterm infants at risk for bronchopulmonary dysplasia. Am J Respir Crit Care Med 2015; 191:87-95.
74. Laughon MM, Langer JC, Bose CL, Smith PB, Ambalavanan N, Kennedy KA, et al. Prediction of bronchopulmonary dysplasia by postnatal age in extremely premature infants. Am J Respir Crit Care Med 2011; 183:1715-22.
75. Nyp M, Sandritter T, Poppinga N, Simon C, Truog WE. Sildenafil citrate, bronchopulmonary dysplasia and disordered pulmonary gas exchange: any benefits? J Perinatol 2012; 32:64-9.
76. Bhat R, Salas AA, Foster C, Carlo WA, Ambalavanan N. Prospective analysis of pulmonary hypertension in extremely low birth weight infants. Pediatrics 2012; 129:e682-9.
77. Laughon M, Allred EN, Bose C, O'Shea TM, Van Marter LJ, Ehrenkranz RA, et al. Patterns of respiratory disease during the first 2 postnatal weeks in extremely premature infants. Pediatrics 2009; 123:1124-31.

FIGURE LEGENDS

Figure 1. Neonatal hyperoxia promotes AHR, mucus production and type 2 airway inflammation.
(A) Experimental schemes. Neonatal mice were exposed to hyperoxia or RA for 7 days and then housed in RA until PN28 for analysis of AHR, histology and lung inflammation.
(B) Airway resistance (RL) was determined following methacholine challenge in mice exposed to RA or O2. n=5 or 6 mice per group (mean ± SEM).
(C) Lung sections were stained with hematoxylin and eosin (H&E) or periodic acid-Schiff (PAS).
(D) Pathology scores on PAS staining sections were quantified. n=13 or 14 mice per group (mean ± SEM).
(E) % of PAS-positive areas within airway epithelium was calculated by image analysis. n=13 or 14 mice per group (mean ± SEM).
(F) Lung mucus associated genes were measured by quantitative RT-PCR. n=3 or 4 mice per group (mean ± SEM).
(G) Lung cytokine gene expressions were determined by quantitative RT-PCR. n=6 mice per group (mean ± SEM).
(H) The frequencies and absolute numbers of eosinophils (CD45+SiglecF+CD11c-) in BAL were measured by flow cytometry. n=3 mice per group (mean ± SEM).
(I) The frequencies and absolute numbers of neutrophils (CD45+Ly6G+CD11b+) in BAL were measured by flow cytometry. n=3 mice per group (mean ± SEM).
Data are representative of at least three independent experiments. n.s., not significant; * $P \leq 0.05$.

Figure 2. Neonatal hyperoxia promotes ILC2 responses.
Mice were exposed to RA or O2 as in Fig. 1A
(A) Representative FACS plot of IL-13-producing cells in the lungs.
(B and C) The frequencies of IL-13+ cells in CD4- (B) or Lin- (C) were determined by flow cytometry. n=3 mice per group (mean ± SEM).
(D) Expression of surface markers on ILC2s (Lin-CD25+CD127+) in mice exposed to RA or O2.
(E) The frequencies and absolute numbers of ILC2s in the lungs were measured at the indicated PN days. n=3 to 7 mice per group (mean ± SEM) (mean ± SEM).
Data are representative of at least two independent experiments. n.s., not significant; * $P \leq 0.05$.

Figure 3. AHR development and pulmonary type 2 inflammation following neonatal hyperoxia are

mediated by ILC2s.

(A) Neonatal mice were exposed to RA or O2 as in Fig. 1A and airway resistance (RL) was determined at PN 28. n=4 to 11 mice per group (mean ± SEM).

(B and C) Lung sections were stained with H&E (B) or PAS (C).

(D) Pathology scores on PAS staining sections were quantified. n=9 or 10 mice per group (mean ± SEM).

(E) % of PAS-positive areas within airway epithelium was calculated by image analysis. n=9 or 10 mice per group (mean ± SEM).

(F) The frequencies and absolute numbers of airway eosinophils were measured by flow cytometry. n=4 mice per group (mean ± SEM).

Data are representative of at least two independent experiments. n.s., not significant; * $P \leq 0.05$.

Figure 4. Neonatal hyperoxia enhances Th2 response to subsequent HDM exposure.

(A) Experimental scheme. Mice exposed to RA or O2 were exposed to HDM for 4 weeks from PN28 to PN56.

(B) BAL cell counts, BAL eosinophil and neutrophil numbers were determined by flow cytometry. n=3 to 5 mice per group (mean ± SEM).

(C) Airway cytokine producing cells were measured by intracellular staining. n=3 or 4 mice per group (mean ± SEM).

(D) Representative FACS plot of cytokine-producing cells in the airway.

Data are representative of at least two independent experiments. * $P \leq 0.05$.

Figure 5. Oxidative stress-dependent IL-33 production is associated with enhanced ILC2 responses following neonatal hyperoxia.

(A) Lung cytokine gene expression levels were measured by quantitative RT-PCR at PN7 or PN14. n=3 to 5 mice per group (mean ± SEM).

(B) Cytokine protein levels were determined by ELISA in the lung supernatants at PN21. n=3 mice per group (mean ± SEM).

(C) MLE-12 cells were exposed to different concentrations of H2O2. Il33 gene expression was determined by quantitative RT-PCR. n=2 per group (mean ± SEM).

(D) MLE-12 cells were exposed to H2O2 of 200 μM in the presence or absence of sulforalphane (SFN) and Il33 gene expression was determined by quantitative RT-PCR. n=2 per group (mean ± SEM).

(E) MLE-12 cells were cultured under normoxia or hyperoxia condition for 24 hours in the presence or absence of SFN and then recovered in normoxia incubator for additional 24 hours. Il33 expression was

determined by quantitative RT-PCR. n=3 per group (mean ± SEM).
(F) Neonatal mice were exposed to RA or O2 and treated with SFN. IL-33 protein levels were measured at PN21. n=2 or 3 mice per group (mean ± SEM).
(G, H) Neonatal mice were exposed to RA or O2 and treated with SFN. Total ILC2 (G) or IL-13+ ILC2 numbers were determined at PN28. n=4 or 8 mice per group (mean ± SEM).
Data are representative of at least two independent experiments. n.s., not significant; * $P \leq 0.05$.

Fig. 6. Asthma-related gene expression and ILC2 responses are mediated by IL-33 signaling.
(A) Lung asthma-related genes were measured by the mouse asthma and allergy RT2 PCR array at PN28.
(B) Il5, Il13, Il21, arg1, Rnase2a and Pmch genes were confirmed by real-time PCR. n=3 or 4 mice per group (mean ± SEM).
(C) ILC2s in the lungs of WT or ST2-deficient mice were measured by flow cytometry at PN28. n=3 or 4 mice per group (mean ± SEM).
(D) Representative FACS plots and absolute numbers of IL-13 or IL-5 producing cells in the lungs of WT or ST2-deficient mice following RA or O2 exposure at PN28. n=2 or 4 mice per group (mean ± SEM).
(E) The frequencies and absolute numbers of eosinophils in the airway of WT or ST2-deficient mice were determined by flow cytometry at PN28. n=3 or 4 mice per group (mean ± SEM).
Data are representative of at least two independent experiments. n.s., not significant; * $P \leq 0.05$.

Fig. 7. Serum IL-33 levels correlate with IL-5 and IL-13 levels in preterm infants.
IL-33, IL-5, IL-13 and IL-4 cytokine levels in the sera of preterm infants were measured by multiplex. Correlations between IL-33 and IL-5 (A), IL-13 (B) or IL-4(C) were evaluated by Pearson's test using GraphPad Prism.

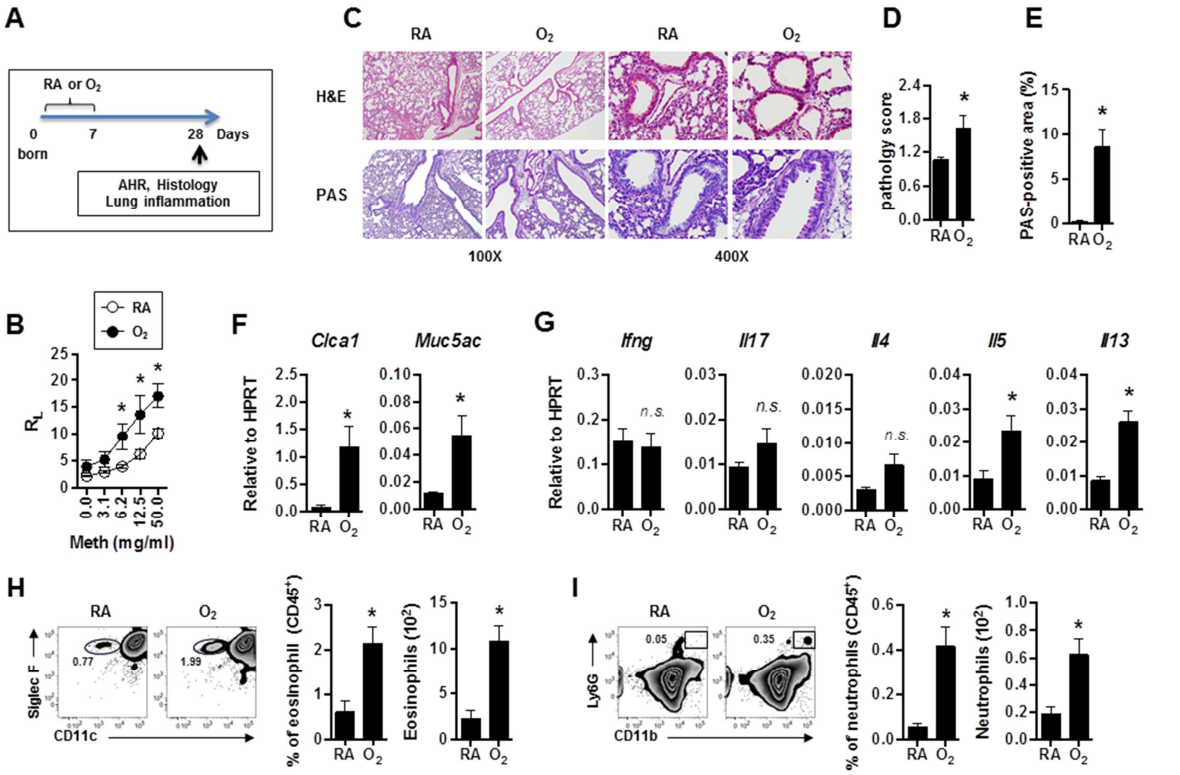

Fig.1

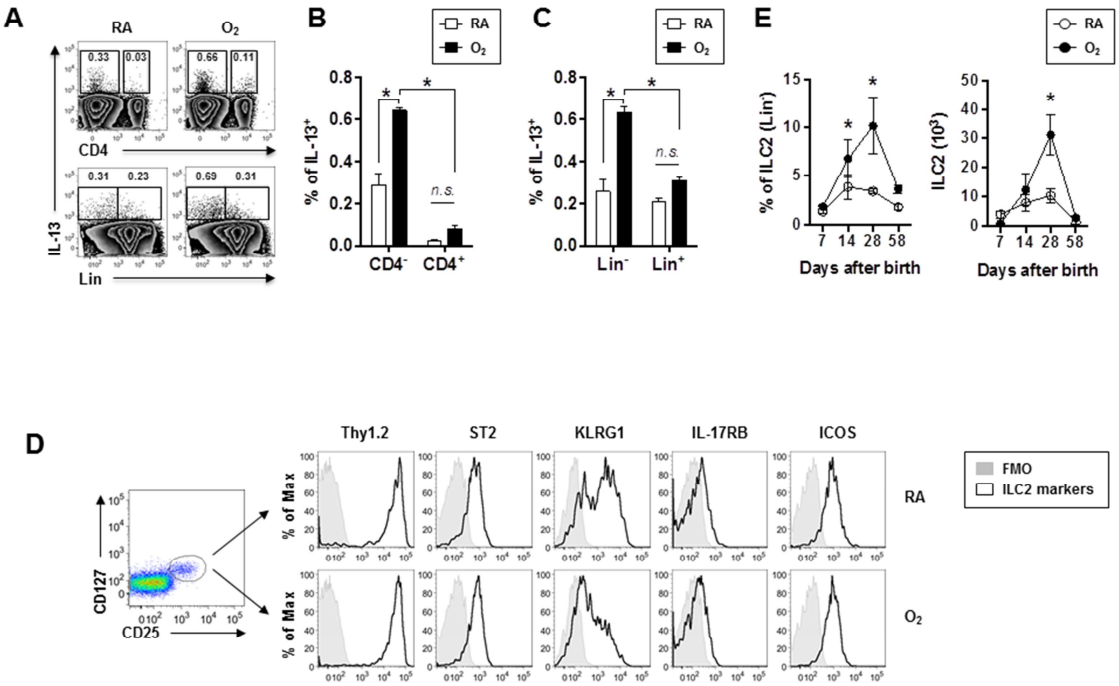

Figure 2

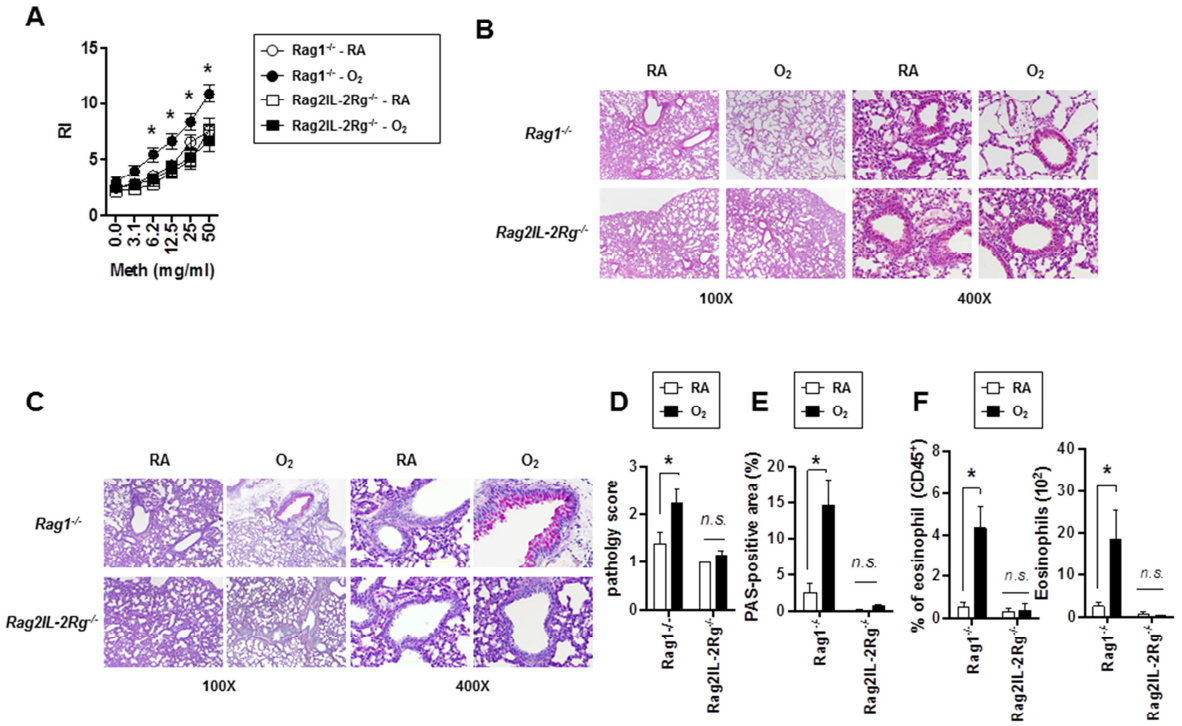

Fig.3

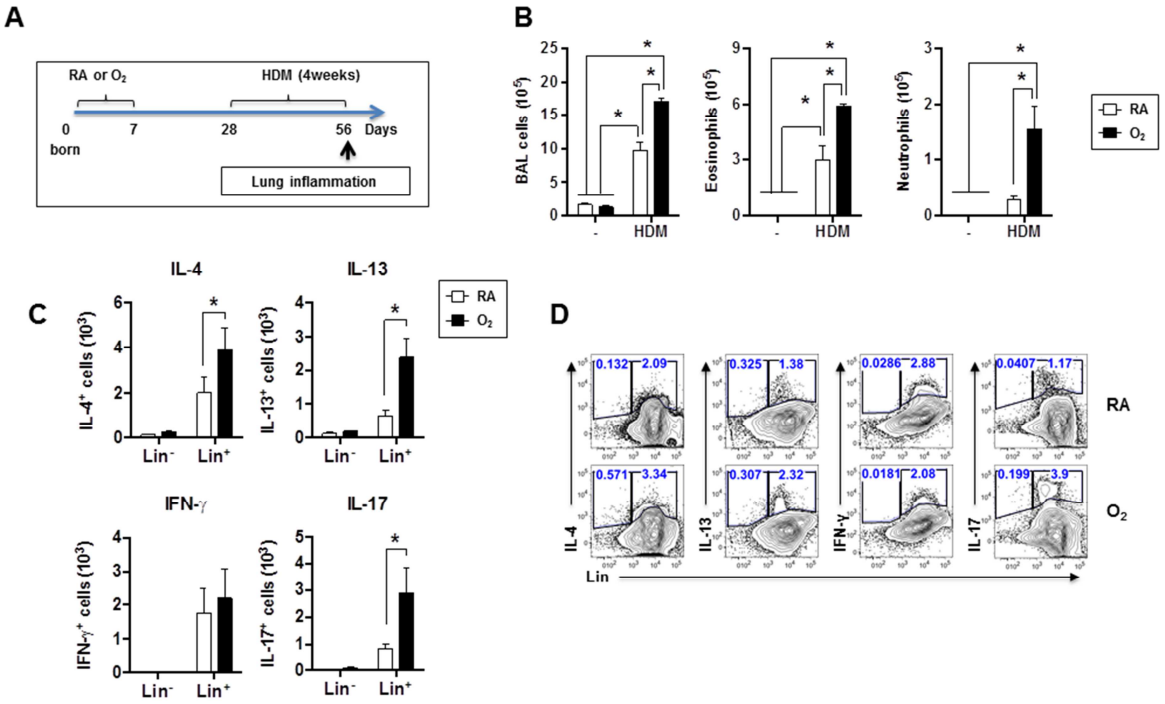

Figure 4

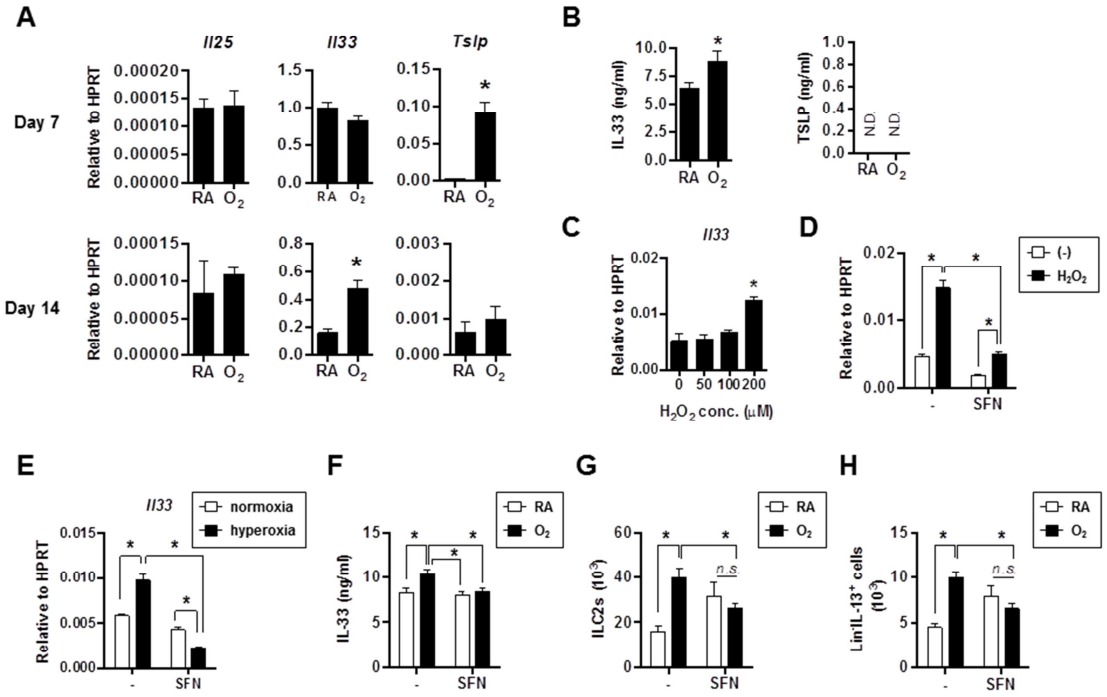

Figure 5

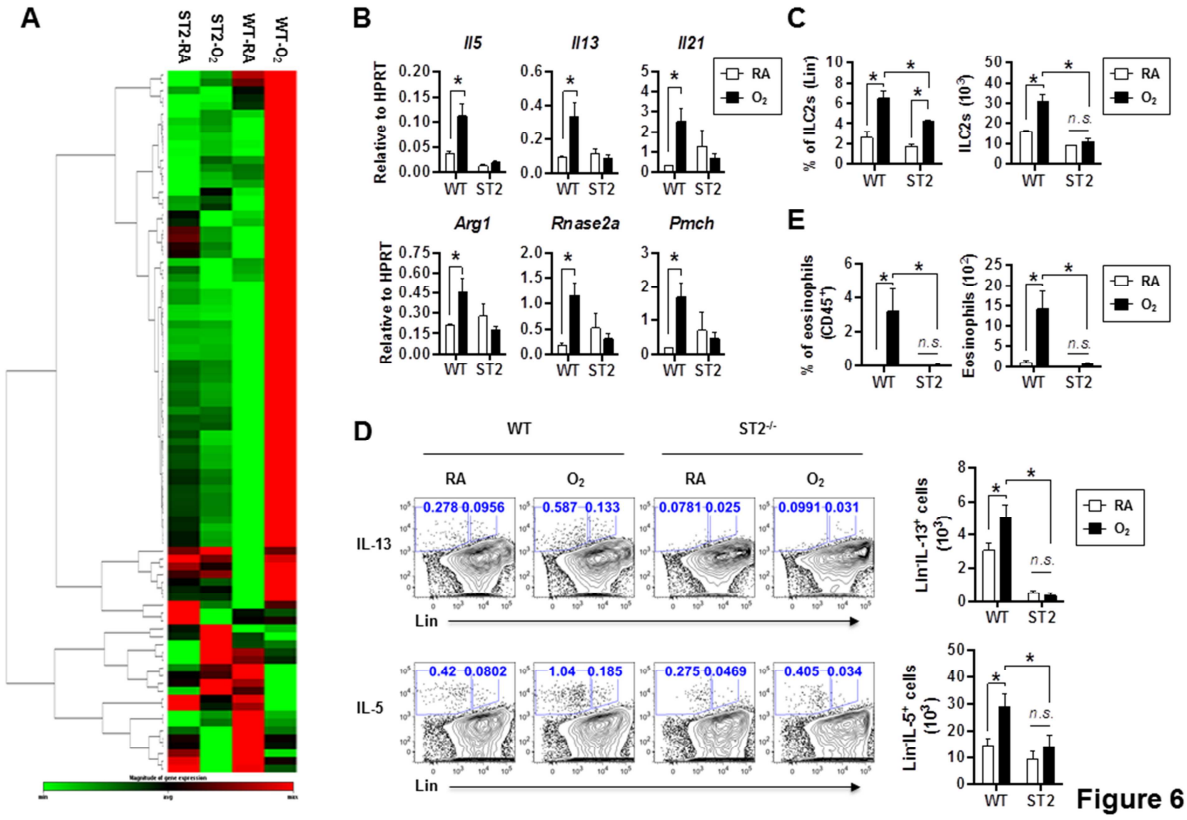

Figure 6

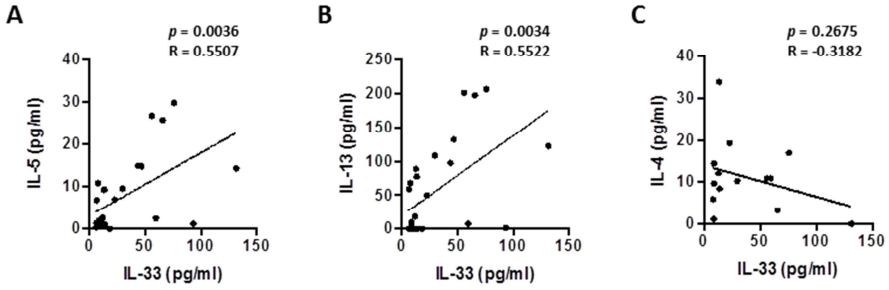

Figure 7

SUPPLEMENTARY FIGURE LEGENDS

Supplementary Fig. 1. Gating strategy of ILC2s

Lung single cells were isolated and stained with Lin (CD11b, CD11c, CD3, Gr-1, B220, TCRβ, Ter-119, NK1.1), ST2, CD90, CD25 and CD127. ILC2s were defined as Lin^- $CD25^+$ $CD127^+$.

Supplementary Fig. 2. Quantification of certain innate cell populations in the lungs of RA or O_2-exposed mice.

Neonatal mice were exposed to RA or O_2 for 7 days. Total DCs, $Fc\varepsilon RI^+$ DCs, mast cells and basophils were quantified in the lungs at PN28. n=3 or 4 mice per group (mean ± SEM). * $P \leq 0.05$.

Supplementary Fig. 3. Cytokine producing cells in the lungs of RA or O_2 exposed-mice following HDM challenge.

Cytokine producing cells in the lungs were measured by intracellular staining. n=4 mice per group (mean ± SEM). * $P \leq 0.05$.

Supplementary Fig. 4. Absolute numbers and frequencies of ILC2s in the lungs of RA or O_2 exposed-mice following chronic HDM challenge

Mice were exposed to RA or O_2 and challenged with HDM as in Fig. 4. Numbers or frequencies of ILC2s in the lungs were determined by flow cytometry at PN56. n=4 mice per group (mean ± SEM).

Supplementary Fig.5. Neonatal hyperoxia promotes oxidative stress in the lungs.

Neonatal mice were exposed to RA or O_2 for 7 days and then housed in RA. (A) ROS levels in lung epithelial cells of RA or O_2- exposed mice were determined by H2DCFDA staining at PN21. n=3 to 5 mice per group (mean ± SEM). * $P \leq 0.05$. (B) Oxidative stress genes in the lungs of RA, O_2- exposed or SFN-treated O_2- exposed mice were measured through mouse oxidative stress RT^2 PCR array at PN15.

Supplementary Fig. 6. IL-33 signaling enhances allergy and asthma gene expression.
Gene expression fold changes were compared between indicated two groups. (A) WT RA group v.s. O_2 group. (B) ST2-deficient RA v.s. O_2 groups. (C) WT O_2 group v.s. ST2 deficient O_2 group.

Supplementary Fig. 7. Serum cytokine levels in Term or Preterm infants.
Human sera from term or preterm infants were collected. IL-33, IL-5, IL-13 and IL-4 levels were determined by multiplex. (A) The levels of cytokines were represented by column graph. (B and C) Pie charts of the frequencies of indicated serum IL-33 concentration ranges in the groups of term infant, pre-term infant with or without BPD criteria (B), or in the groups of infants born before 30 weeks of gestational age, between 30 to 37 gestational age or over 37 gestational age (C).

Supplementary Fig. 8. Correlation analysis of serum IL-33 and IL-13, and serum IL-33 and IL-5 in term infants.
Correlations between serum IL-33 and IL-5 or serum IL-33 and IL-13 were evaluated by Pearson's test using GraphPad Prism.

Supplementary Fig. 9. Correlation analysis of serum IL-33 and IL-13, and serum IL-33 and IL-5 according to infant age groups.
Correlations between serum IL-33 and IL-5 or serum IL-33 and IL-13 in samples collected from infants younger than 18 months or infants between 18 months and 30 months of age were evaluated by Pearson's test using GraphPad Prism.

Term

	gender	gestational age (weeks)	age (mo)	IL-33 (pg/ml)	IL-13 (pg/ml)	IL-5 (pg/ml)	IL-4 (pg/ml)
1	M	40	7.6	1.85	*n.d.*	0.5	*n.d.*
2	F	38	14.5	26.18	29.12	4.15	*n.d.*
3	F	38	14.5	10.87	143.37	17.28	0.47
4	F	40	21.8	15.54	38.27	4.41	*n.d.*
5	M	39	14.2	4.22	11.68	1.24	*n.d.*
6	F	40	3.4	2.64	*n.d.*	0.84	3.35
7	F	39	18.9	26.76	174.24	26.73	24.38
8	M	38	6.3	*n.d.*	*n.d.*	3.29	*n.d.*
9	M	38	6.5	5.8	*n.d.*	0.97	15.75
10	M	40	27.0	36.4	48.27	5.85	*n.d.*
11	F	40	25.2	*n.d.*	94.54	14.99	5.98
12	F	40	25.1	0.45	*n.d.*	*n.d.*	*n.d.*
13	F	40	8.8	*n.d.*	*n.d.*	0.3	*n.d.*
14	F	39	11.4	2.84	*n.d.*	1.24	*n.d.*
15	F	40	29.0	5.8	*n.d.*	0.02	*n.d.*
16	M	40	10.1	0.65	*n.d.*	2.17	*n.d.*

	gender	gestational age (weeks)	age (mo)	IL-33 (pg/ml)	IL-13 (pg/ml)	IL-5 (pg/ml)	IL-4 (pg/ml)
1	M	35	16.17	4.22	34.93	4.67	*n.d.*
2	F	32	7.87	*n.d.*	*n.d.*	0.3	*n.d.*
3	F	32	7.87	*n.d.*	*n.d.*	*n.d.*	*n.d.*
4	M	32	7.87	9.12	*n.d.*	2.04	9.74
5	F	30	9.50	8.34	*n.d.*	1.1	5.98
6	M	35	11.97	6.38	*n.d.*	0.43	*n.d.*
7	F	32	12.37	4.22	8.62	1.64	*n.d.*
8	F	32	12.37	3.83	33.8	3.09	*n.d.*
9	F	32	12.87	8.93	1.73	1.1	*n.d.*
10	M	32	12.87	3.44	5.62	1.24	*n.d.*
11	F	28	23.80	8.53	*n.d.*	1.5	*n.d.*
12	F	28	23.80	5.4	3.23	2.3	13.38
13	M	31	18.40	46.8	132.37	14.86	*n.d.*
14	M	34	12.70	*n.d.*	*n.d.*	1.17	*n.d.*
15	F	30	15.20	13.01	89.07	9.38	12.18
16	M	31	21.33	*n.d.*	23.53	3.22	*n.d.*
17	M	32	11.80	3.83	*n.d.*	2.5	3.35
18	F	31	14.10	2.25	*n.d.*	0.84	*n.d.*
19	F	31	14.50	*n.d.*	14.46	2.83	*n.d.*
20	M	35	22.50	*n.d.*	*n.d.*	1.1	*n.d.*
21	F	34	15.53	43.72	97.65	14.99	*n.d.*
22	M	34	22.23	29.85	108.66	9.65	10.36
23	F	30	19.23	*n.d.*	*n.d.*	*n.d.*	*n.d.*
24	M	30	19.23	*n.d.*	*n.d.*	0.7	*n.d.*
25	M	32	11.60	3.24	*n.d.*	0.84	*n.d.*
26	M	35	21.40	4.22	4.49	1.64	*n.d.*
27	F	35	21.40	11.26	*n.d.*	1.77	*n.d.*
28	M	29	14.53	4.42	*n.d.*	1.24	9.13
29	M	29	14.53	5.6	*n.d.*	0.84	*n.d.*
30	F	33	8.03	*n.d.*	*n.d.*	*n.d.*	*n.d.*
31	M	33	8.03	*n.d.*	*n.d.*	*n.d.*	*n.d.*
32	M	33	13.07	3.1	*n.d.*	*n.d.*	*n.d.*
33	M	31	12.10	9	9.72	1.78	14.47
34	M	30	23.33	131.56	122.59	14.33	0.12

	gender	tational age (wee	age (mo)	IL-33 (pg/ml)	IL-13 (pg/ml)	IL-5 (pg/ml)	IL-4 (pg/ml)
1	F	24	20.07	1.45	*n.d.*	0.02	*n.d.*
2	F	24	20.10	1.45	*n.d.*	1.5	*n.d.*
3	M	26	27.53	*n.d.*	*n.d.*	0.02	*n.d.*
4	F	28	15.07	3.04	*n.d.*	0.16	*n.d.*
5	M	29	25.53	93.18	1.73	1.24	*n.d.*
6	F	24	25.50	12.04	18.49	2.7	*n.d.*
7	F	25	23.43	4.81	*n.d.*	0.7	*n.d.*
8	F	24	19.47	18.25	*n.d.*	*n.d.*	*n.d.*
9	F	30	6.97	*n.d.*	*n.d.*	0.7	*n.d.*
10	F	28	22.50	56.03	201.56	26.86	10.97
11	F	28	22.50	3.04	*n.d.*	0.57	*n.d.*
12	F	29	19.87	2.64	*n.d.*	1.1	*n.d.*
13	M	26	18.47	6.58	*n.d.*	1.37	*n.d.*
14	M	25	20.63	0.25	*n.d.*	*n.d.*	*n.d.*
15	M	26	24.10	1.65	*n.d.*	1.37	0.47
16	M	26	18.37	6.58	59.33	6.84	*n.d.*
17	F	33	13.03	2.25	*n.d.*	1.64	*n.d.*
18	M	26	23.60	22.9	50.29	7.03	19.24
19	F	24	25.07	59.69	7.67	2.5	10.97
20	F	26	25.53	75.66	207.14	29.87	16.92
21	F	25	17.37	*n.d.*	*n.d.*	1.5	*n.d.*
22	M	28	10.33	*n.d.*	*n.d.*	0.77	*n.d.*
23	F	28	8.23	1.85	*n.d.*	0.43	*n.d.*
24	F	27	24.40	13.99	*n.d.*	1.1	8.51
25	F	27	24.70	1.85	*n.d.*	1.24	*n.d.*
26	M	27	18.53	13.6	77.84	9.38	33.84
27	M	26	19.77	65.65	198.06	25.82	3.35
28	M	24	12.73	2.25	*n.d.*	2.96	14.56
29	M	27	13.03	5.8	*n.d.*	3.36	*n.d.*
30	M	26	10.27	3.04	*n.d.*	1.64	*n.d.*
31	M	29	18.57	8.93	*n.d.*	0.7	1.24

Pre-term no BPD

	gender	gestational age (weeks)	age (mo)	IL-33 (pg/ml)	IL-13 (pg/ml)	IL-5 (pg/ml)	IL-4 (pg/ml)
1	M	35	16.17	4.22	34.93	4.67	*n.d.*
2	F	32	7.87	*n.d.*	*n.d.*	0.3	*n.d.*
3	F	32	7.87	*n.d.*	*n.d.*	*n.d.*	*n.d.*
4	M	32	7.87	9.12	*n.d.*	2.04	9.74
5	F	30	9.50	8.34	*n.d.*	1.1	5.98
6	M	35	11.97	6.38	*n.d.*	0.43	*n.d.*
7	F	32	12.37	4.22	8.62	1.64	*n.d.*
8	F	32	12.37	3.83	33.8	3.09	*n.d.*
9	F	32	12.87	8.93	1.73	1.1	*n.d.*
10	M	32	12.87	3.44	5.62	1.24	*n.d.*
11	F	28	23.80	8.53	*n.d.*	1.5	*n.d.*
12	F	28	23.80	5.4	3.23	2.3	13.38
13	M	31	18.40	46.8	132.37	14.86	*n.d.*
14	M	34	12.70	*n.d.*	*n.d.*	1.17	*n.d.*
15	F	30	15.20	13.01	89.07	9.38	12.18
16	M	31	21.33	*n.d.*	23.53	3.22	*n.d.*
17	M	32	11.80	3.83	*n.d.*	2.5	3.35
18	F	31	14.10	2.25	*n.d.*	0.84	*n.d.*
19	F	31	14.50	*n.d.*	14.46	2.83	*n.d.*
20	M	35	22.50	*n.d.*	*n.d.*	1.1	*n.d.*
21	F	34	15.53	43.72	97.65	14.99	*n.d.*
22	M	34	22.23	29.85	108.66	9.65	10.36
23	F	30	19.23	*n.d.*	*n.d.*	*n.d.*	*n.d.*
24	M	30	19.23	*n.d.*	*n.d.*	0.7	*n.d.*
25	M	32	11.60	3.24	*n.d.*	0.84	*n.d.*
26	M	35	21.40	4.22	4.49	1.64	*n.d.*
27	F	35	21.40	11.26	*n.d.*	1.77	*n.d.*
28	M	29	14.53	4.42	*n.d.*	1.24	9.13
29	M	29	14.53	5.6	*n.d.*	0.84	*n.d.*
30	F	33	8.03	*n.d.*	*n.d.*	*n.d.*	*n.d.*
31	M	33	8.03	*n.d.*	*n.d.*	*n.d.*	*n.d.*
32	M	33	13.07	3.1	*n.d.*	*n.d.*	*n.d.*
33	M	31	12.10	9	9.72	1.78	14.47
34	M	30	23.33	131.56	122.59	14.33	0.12

Pre-term BPD

	gender	gestational age (weeks)	age (mo)	IL-33 (pg/ml)	IL-13 (pg/ml)	IL-5 (pg/ml)	IL-4 (pg/ml)
1	F	24	20.07	1.45	*n.d.*	0.02	*n.d.*
2	F	24	20.10	1.45	*n.d.*	1.5	*n.d.*
3	M	26	27.53	*n.d.*	*n.d.*	0.02	*n.d.*
4	F	28	15.07	3.04	*n.d.*	0.16	*n.d.*
5	M	29	25.53	93.18	1.73	1.24	*n.d.*
6	F	24	25.50	12.04	18.49	2.7	*n.d.*
7	F	25	23.43	4.81	*n.d.*	0.7	*n.d.*
8	F	24	19.47	18.25	*n.d.*	*n.d.*	*n.d.*
9	F	30	6.97	*n.d.*	*n.d.*	0.7	*n.d.*
10	F	28	22.50	56.03	201.56	26.86	10.97
11	F	28	22.50	3.04	*n.d.*	0.57	*n.d.*
12	F	29	19.87	2.64	*n.d.*	1.1	*n.d.*
13	M	26	18.47	6.58	*n.d.*	1.37	*n.d.*
14	M	25	20.63	0.25	*n.d.*	*n.d.*	*n.d.*
15	M	26	24.10	1.65	*n.d.*	1.37	0.47
16	M	26	18.37	6.58	59.33	6.84	*n.d.*
17	F	33	13.03	2.25	*n.d.*	1.64	*n.d.*
18	M	26	23.60	22.9	50.29	7.03	19.24
19	F	24	25.07	59.69	7.67	2.5	10.97
20	F	26	25.53	75.66	207.14	29.87	16.92
21	F	25	17.37	*n.d.*	*n.d.*	1.5	*n.d.*
22	M	28	10.33	*n.d.*	*n.d.*	0.77	*n.d.*
23	F	28	8.23	1.85	*n.d.*	0.43	*n.d.*
24	F	27	24.40	13.99	*n.d.*	1.1	8.51
25	F	27	24.70	1.85	*n.d.*	1.24	*n.d.*
26	M	27	18.53	13.6	77.84	9.38	33.84
27	M	26	19.77	65.65	198.06	25.82	3.35
28	M	24	12.73	2.25	*n.d.*	2.96	14.56
29	M	27	13.03	5.8	*n.d.*	3.36	*n.d.*
30	M	26	10.27	3.04	*n.d.*	1.64	*n.d.*
31	M	29	18.57	8.93	*n.d.*	0.7	1.24

Supplementary figure 1

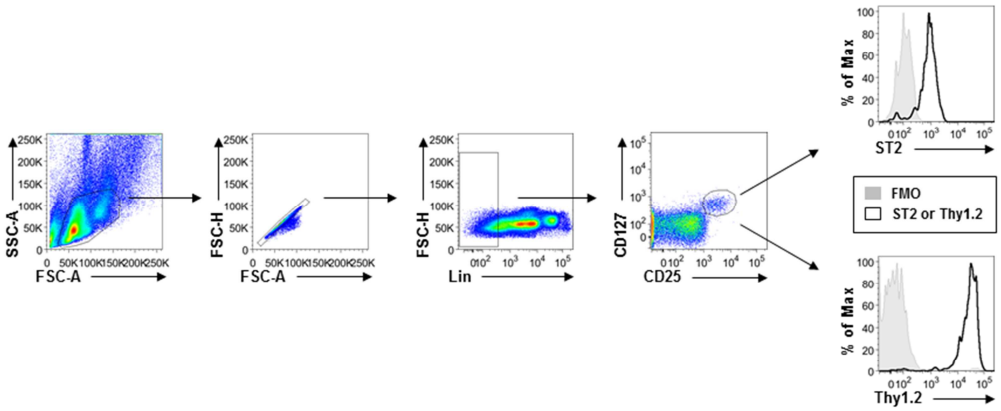

Supplementary figure 2

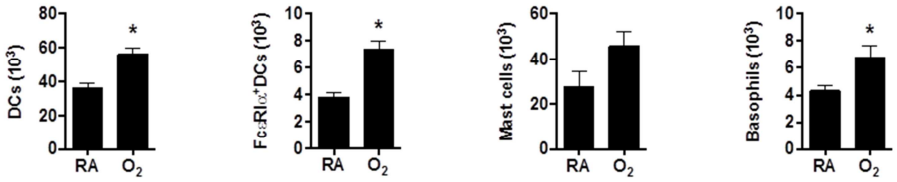

Supplementary figure 3

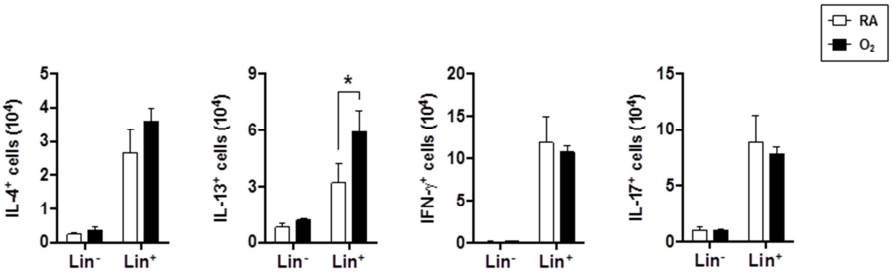

Supplementary figure 4

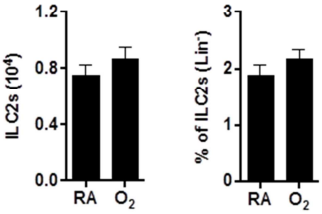

Supplementary figure 5

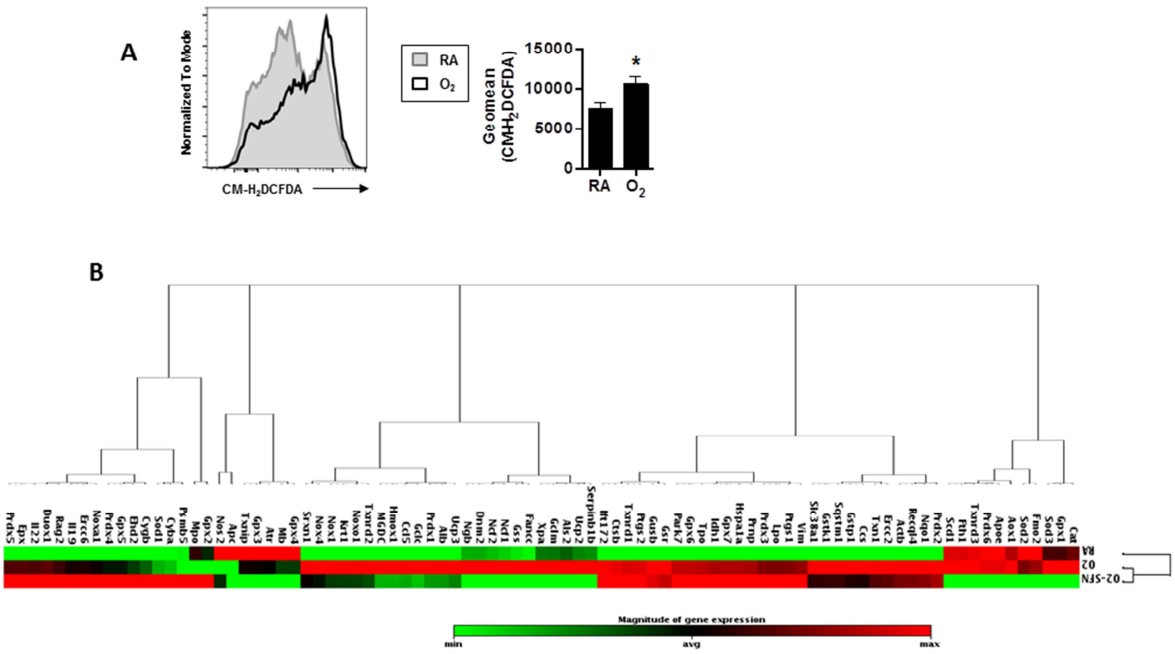

Supplementary figure 6

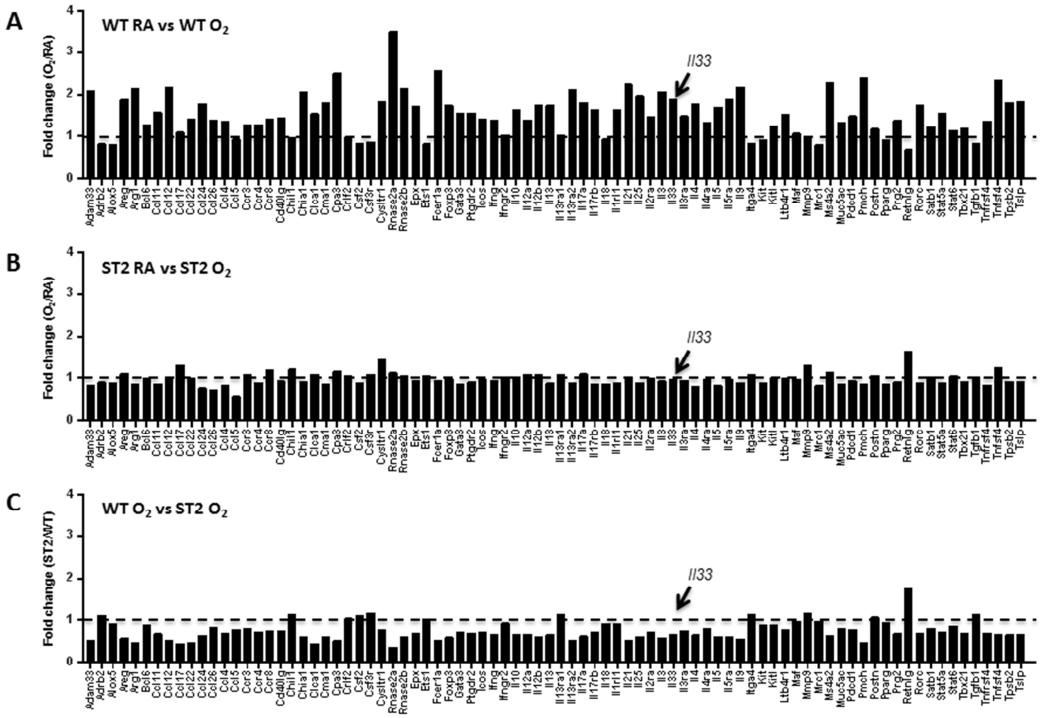

Supplementary figure 7

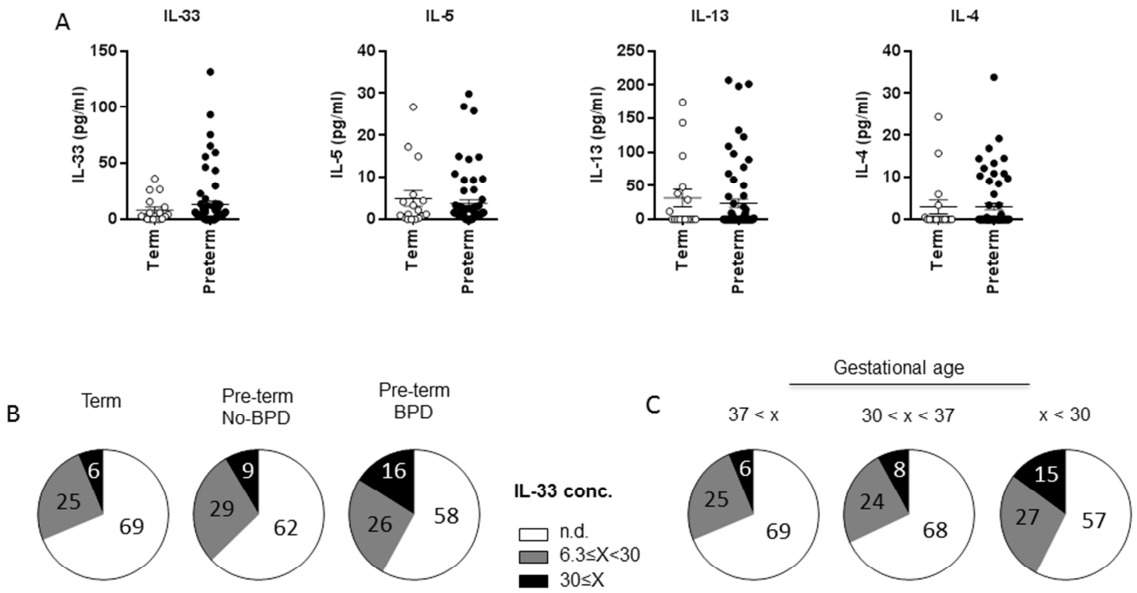

Supplementary figure 8

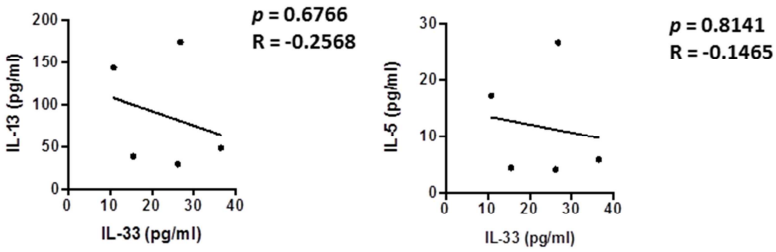

Supplementary figure 9